Univerzita Karlova

1. lékařská fakulta

Studijní program: Biomedicína

Studijní obor: Fyziologie a patofyziologie člověka

UNIVERZITA KARLOVA
1. lékařská fakulta

Mgr. Petr Páral

Buněčný cyklus a diferenciace krvetvorných kmenových a progenitorových buněk

The cell cycle and differentiation of haematopoietic stem and progenitor cells

Disertační práce

Ph.D. Thesis

Vedoucí závěrečné práce/Školitel: RNDr. Luděk Šefc, CSc.

Konzultant: Prof. MUDr. Emanuel Nečas, DrSc.

Praha, 2019

Prohlášení:

Prohlašuji, že jsem závěrečnou práci zpracoval samostatně a že jsem řádně uvedl a citoval všechny použité prameny a literaturu. Současně prohlašuji, že práce nebyla využita k získání jiného nebo stejného titulu.

Souhlasím s trvalým uložením elektronické verze mé práce v databázi systému meziuniverzitního projektu Theses.cz za účelem soustavné kontroly podobnosti kvalifikačních prací.

V Praze, 15.5.2019

Mgr. Petr Páral

Podpis

Identifikační záznam:

PÁRAL, Petr. *Buněčný cyklus a diferenciace krvetvorných kmenových a progenitorových buněk. [The cell cycle and differentiation of haematopoietic stem and progenitor cells].* Praha, 2019. 91 s., 2 příl. Disertační práce (PhD). Univerzita Karlova, 1. lékařská fakulta, Ústav patologické fyziologie. Vedoucí práce RNDr. Luděk Šefc, CSc.

Poděkování:

Na tomto místě bych rád poděkoval svým školitelům, RNDr. Luďkovi Šefcovi, CSc. a Prof. MUDr. Emanuelovi Nečasovi, DrSc. za pomoc s formulováním cílů práce, designem experimentů a za veškerou pomoc, které se mi po celou dobu doktorského studia dostávalo.

V neposlední řadě bych rád poděkoval svým kolegům za pomoc a vytvoření přátelského pracovního prostředí.

Disertační práce byla vytvořena za podpory projektů GAČR 14-25515S a GAČR 17-01897S od Grantové agentury ČR a projektů PROGRES Q26 a SVV 260371 od Univerzity Karlovy.

Content

List of Abbreviations 7
1 Introduction 10
1.1 The cell cycle 10
1.1.1 Cyclins 10
1.1.2 Cyclin-dependent kinases (CDKs) 11
1.1.3 Cyclin-dependent kinase inhibitors (CDKIs) 11
1.1.4 Cell cycle progression 12
1.2 The cell cycle analysis 15
1.2.1 The S-phase cell determination 15
1.2.2 Cell cycle flow rate measurement 17
1.3 Haematopoietic stem and progenitor cells (HSPCs) 20
1.4 Dual EdU-BrdU sequential DNA-labelling technique in the study of haematopoiesis 21
1.5 The cell cycle activity of haematopoietic stem and progenitor cells 22
1.6 Quantification of murine haematopoiesis 23
1.7 Erythropoiesis 25
1.7.1 Embryonal erythropoiesis 25
1.7.2 Adult erythropoiesis 26
1.7.3 Identification of erythroid progenitors and precursors 28
1.7.4 S-phase specific erythroid differentiation 29
2 Hypothesis 30
Aims of the study 30
3 Materials and Methods 32
3.1 Materials 32
3.1.1 Chemicals 32
3.1.2 Antibodies 33
3.1.3 Buffers 36
3.2 Instruments and software 37
3.3 Experimental animals 38
3.4 Bone marrow collection 38
3.5 Immunophenotyping of cell populations 38
3.6 Cell cycle analysis 39
3.6.1 Percentage of DNA-synthesizing cells determined by *in vitro* staining 39
3.6.2 Cell cycle analysis after *in vivo* staining of DNA synthesizing cells 39
3.7 Flow cytometry and cell sorting 41

3.8 Imaging flow cytometry 41
3.9 *In vitro* cultivation of erythroid progenitors in semi-solid media 41
3.10 Statistical analysis 42
4 Results 43
4.1 Determination of DNA synthesizing cell fraction in HSPC subpopulations 43
4.1.1 Flow cytometry analysis of HSPC subpopulations 43
4.1.2 The fraction of DNA-synthesizing cells is a characteristic feature of HSPC subpopulations 44
4.1.3 The HSPC proliferation hierarchy is age and sex independent 45
4.2 Cell cycle kinetics in HSPC subpopulations 46
4.2.1 Refinement of the EdU-BrdU technique for determination of the HSPC cell flow rate into the G2-phase of the cell cycle 46
4.2.2 Cell flow rate into the G2-phase and S-phase duration in HSPCs 50
4.2.3 Cell cycle duration in HSPCs 52
4.2.4 Cell flow rate of DNA labelled cells arising from mitosis 53
4.2.5 Cell numbers generated by mitotic division do not correspond to the number of cells entering G2-phase 55
4.2.6 Estimation of cell production in HSPCs 56
4.3 Cell cycle and differentiation of erythroid progenitor and precursor cells 58
4.3.1 Imaging flow cytometry analysis of erythroid progenitor and precursor cells 58
4.3.2 Progression of erythroid progenitor and precursor cells through S-phase of the cell cycle and its association with cell differentiation 62
4.3.3 Dynamic cell cycle analysis in cells initiating the erythroid developmental pathway 65
5 Discussion 69
5.1 Cell cycle and cell cycle kinetics of HSPCs 69
5.2 Erythroid developmental pathway in mouse bone marrow analysed by flow cytometry 73
6 Conclusions 77
7 Summary 78
8 Souhrn 79
9 Key words 80
10 Klíčová slova 80
11 References 81
12 List of Publications 90
13 Appendices 91

List of Abbreviations

7-AAD	7-aminoactinomycin D
AGM	aorta gonad mesonephros
a-HSCs	active haematopoietic stem cells
ANOVA	analysis of variance
APC	allophycocyanin
APC/C	anaphase-promoting complex/cyclosome
APC/Cy7	allophycocyanin/cyanin 7
APC/Fire ™ 750	allophycocyanin/Fire ™ 750
BasoE	basophilic erythroblasts
BFU-E	burst-forming unit-erythroid
BMCs	bone marrow cells
BrdU	5-bromo-2´-deoxy-uridine
BSA	bovine serum albumin
CDKs	cyclin dependent kinases
CDKIs	cyclin-dependent kinase inhibitors
CFU-E	colony-forming unit-erythroid
CIP/KIP	CDK interacting protein/Kinase inhibitory protein
c-Kit	CD117, stem cell factor receptor
CLPs	common lymphoid progenitors
CMPs	common myeloid progenitors
d-HSCs	dormant haematopoietic stem cells
E+B+	EdU and BrdU double-labelled cells
E+B-	EdU single labeled cells
E-B+	BrdU single-labelled cells
EdU	5-ethenyl-2´-deoxyuridine
Epo	erythropoietin
EryP-CFC	primitive erythroid colony-forming cells
FACS	fluorescence-activated cell sorting
FOG-1	friend-of-GATA-1
FITC	fluorescein isothiocyanate

FMO	fluorescence minus one
GFP	green fluorescent protein
GM-CSF	granulocyte-macrophage colony-stimulating factor
GMPs	granulocyte-macrophage progenitors
Gwl	Greatwall kinase
H2B	histone2B
HPCs	heterogeneous restricted progenitors
HSCs	haematopoietic stem cells
HSPCs	haematopoietic stem and progenitor cells
I+	cells labelled only with IdU
I+B+	cells double-labelled with IdU and BrdU
IdU	5-iodo-2´-deoxy-uridine
IGF-1	insulin-like growth factor 1
IL-3	interleukin 3
IL7R	interleukin 7 receptor
IMDM	Iscove's Modified Dulbecco's Medium
INK4	inhibitors of CDK4 and of CDK6
Lin	lineage
LSK	$Lin^{-}c\text{-}Kit^{+}Sca\text{-}1^{+}$
LS^{-}K	$Lin^{-}c\text{-}Kit^{+}Sca\text{-}1^{-}$
MEPs	megakaryocyte-erythroid progenitors
MPF	M-phase promoting factor
MPPs	multipotent progenitors
OrthoE	orthochromatic erythroblasts
PBS	phosphate buffered saline
PE	phycoerythrin
PE/Cy7	phycoerythrin/cyanin 7
PI	propidium iodide
PolyE	polychromatophilic erythroblasts
pRb	retinoblastoma protein
ProE	proerythroblasts
R	ratio

RBCs	red blood cells
R-point	restriction point
Sca-1	stem cell antigen
SCF	S-phase kinase-associated protein (Skp-1)/Cullin/F-box protein
SCF	stem cell factor
SD	standard deviation
SEM	atandard error of the mean
SDF-1	stromal cell-derived factor 1
SLAM	signalling lymphocytic activation molecule, surface molecules CD150 and CD48
YFP	yellow fluorescent protein

1 Introduction

1.1 The cell cycle

The cell lifespan starts at the moment that the parental cell divides and completes when the cell undergoes mitosis. The cell cycle is comprised of the sequence of events that take place between two consecutive mitoses and results in the formation of the two daughter cells. The cell cycle consists of two stages: 1) interphase and 2) M-phase (mitosis) followed by cytokinesis. Interphase represents the period when a cell is metabolically active, grows, transcribes genes, synthesizes proteins, carries out its functions depending on its specialization in a multicellular organism, differentiates, replicates nuclear DNA and prepares itself for a mitotic division. Interphase is in terms of the cell division divided into three phases: G1 (Gap 1)-, S (Synthesis)-, and G2 (Gap 2)-phase. During the G1-phase, the cell increases the volume of the cytoplasm and synthesizes a range of proteins such as the histones and enzymes required for the replication of DNA. The S-phase represents the part of the cell cycle in which DNA replication occurs. The G2-phase follows the S-phase, the cell duplicates the organelles and prepares for mitosis. The M-phase, mitosis, is the final phase of the cell cycle, during which the duplicated chromosomes segregate into the daughter cells. The physical splitting of the dividing cell into the two daughter cells is called cytokinesis.

Progression through the cell cycle, which represents the precise timing of finishing one and entering the next phase, is primarily regulated by two protein families: 1) cyclins and 2) cyclin-dependent kinases (CDKs). Each CDK binds to a different class of cyclins and gives rise to the heterodimeric **cyclin-CDK complex** with the protein kinase activity necessary for activating the numerous substrates required for progression through the phases of the cell cycle (Morgan, 1997).

1.1.1 Cyclins

Cyclins are a large protein family with approximately 30 members in eukaryotes. Cyclins share a homologous region of about 100 amino acid residues called the cyclin box. This region is required for CDK binding, activation of the cyclin-CDK complex (Horton and Templeton, 1997) and also for the proteasome-mediated degradation of some cyclins (Piscopo and Hinds, 2008). A comparative and phylogenetic analysis of eukaryotic cyclins enabled dividing them into

three groups. Group I includes cyclins A, B, D, E, F, G, J, I, O, some of which play a key role in regulating the progression of the cell cycle. Group II contains cyclin Y, which was discovered to be the regulator of Wnt/β-catening signalling in Xenopus embryos, and the group III cyclins C, H, K, L and T, which participate in the regulation of the transcription mediated by RNA polymerase II (Bregman, Pestell and Kidd, 2000; Davidson *et al.*, 2009; Ma *et al.*, 2013). The changes (oscillations) in the protein level of cyclins in group I, especially cyclins A, B, D and E, are cell cycle phase specific and drive the passage through the cell cycle. In other words, the precise timing of the specific cyclin expression and also its degradation in the proteasome enable passage through the cell cycle. According to this phase specificity, cyclins can be divided into G1 cyclins (cyclin D), G1/S cyclins (cyclin E), S cyclins (cyclin A) and G2/M cyclins (cyclins A, B).

1.1.2 Cyclin-dependent kinases (CDKs)

CDKs are a family of serine/threonine protein kinases. Without cyclin binding, CDKs possess no enzymatic activity, when activated by their association with cyclins, they serve as the catalytic subunits of this complex. The number of CDK family members varies between species and reaches up to 20 in mice or humans. But only some of these CDKs are required for the direct regulation of cell cycle progression. CDK4 and CDK6 regulate the exit from the G1 phase, CDK2 participates in the G1 to S-phase transition and in the induction of DNA replication, and CDK1 serves as the mitotic CDK (Malumbres and Barbacid, 2005; Malumbres, 2014). However, the phase specificities of these CDKs are not general and can overlap and also be tissue specific. Berthet et al. (2003) showed that CDK2 knock-out mice are viable, but sterile. Malumbres et al. (2004) proved that CDK6 knock-out mice survive but with defects in haematopoiesis such as a reduction of thymic and splenic size, and that the deletion of both CDK4 and CDK6 resulted in embryonic lethality probably because of the defects in erythropoiesis.

1.1.3 Cyclin-dependent kinase inhibitors (CDKIs)

Other important proteins involved in the cell cycle are negative regulators of the cyclin-CDK complex: CDKIs. CDKIs represent the intrinsic cell cycle control system monitoring proper

passage through the phases of the cell cycle. The activated CDKIs bind directly to the cyclin-CDK complex and thus prevent cell cycle progression.

CDKIs include 2 classes of cell cycle regulators: 1) the INK4 family (p15, p16, p18, p19), which bind CDK4 and CDK6 and block the cell in the G1-phase (Cánepa *et al.*, 2007) , 2), and the CIP/KIP family (p21, p27, p57), which interact with cyclin A-, cyclin D, cyclin E-CDK complexes and inhibit them (Nakayama and Nakayama, 1999; Abukhdeir and Park, 2008).

1.1.4 Cell cycle progression

Growth factor stimulation and microenvironmental signalling enables the cell to enter into the new cell cycle leading to the cell division when the restriction point is crossed. The restriction point (R-point), discovered by Pardee (1974), is the specific point in the G1 phase in which the cell commits itself to proceed further through the cell cycle irrespective of external growth factors (Zetterberg and Larsson, 1985).

Cyclin D, whose synthesis is initiated by growth factors during the G1 phase, associates with CDK4 and CDK6. Active cyclin D – CDK4/6 complexes phosphorylate and thus inactivate the retinoblastoma tumor suppressor protein (pRb). The unphosphorylated pRb binds the proteins of the E2F family of transcription factors, and in this complex acts as the repressor of the genes regulated by E2F. Once the pRb is phosphorylated, it dissociates from the E2F and the E2F-regulated gene expression of cyclins E and A is triggered. The newly synthesized cyclin E associates with CDK2 to form active cyclin E-CDK2 complexes, which further phosphorylate and thus complete the inactivation of pRb. This hyperphosphorylation of pRb is the crucial event responsible for passage through the G1 restriction point and for the G1/S phase transition (Hinds *et al.*, 1992; Cobrinik, 2005; Johnson and Skotheim, 2013).

The expression of cyclin A starts together with the expression of cyclin E. Cyclin A accumulates in the nucleus, where it forms the active cyclin A-CDK2 complexes that collaborate with the cyclin E-CDK2 complexes to initiate DNA replication. The cyclin E/CDK2 complexes stimulate the assembly of replication complexes that are then activated by the cyclin A/CDK2 complex. Moreover, the cyclin A/CDK2 complexes inhibit the assembly of new replication complexes and thus ensure that DNA is replicated once per cell cycle (Coverley, Laman and Laskey, 2002; Woo and Poon, 2003).

As soon as the cyclin E is ubiquitinylated via ubiquitin ligase SCF, which is multi-protein complex consisting of the S-phase kinase-associated protein (Skp-1)/Cullin/F-box protein and subsequently degraded in a proteasome shortly after the initiation of the S-phase, the concentration of cyclin A increases during the S-phase (Clurman *et al.*, 1996; Siu, Rosner and Minella, 2012).

Cyclin A accumulates in the G2-phase and besides CDK, 2 can also bind CDK 1. Active cyclin A/CDK1 complexes enhance the cyclin B expression, regulate the proper kinetochore-microtubule attachment in prometaphase and moreover are involved in the activation of M-phase promoting factor (MPF) and thus regulate the G2-M transition and M-phase initiation (Fung, Ma and Poon, 2007; Kabeche and Compton, 2013; Dumitru *et al.*, 2017). Cyclin A is ubiquitinylated via ubiquitin ligase: anaphase-promoting complex/cyclosome (APC/C) and subsequently degraded in the proteasome in promethaphase (den Elzen and Pines, 2001; Geley *et al.*, 2001). Cyclin B is expressed from the early S-phase, during the G2 phase and peaks in the M-phase. Cyclin B associates with CDK1, the active cyclin B/CDK1 complex together with Greatwall kinase (Gwl) constitute MPF, the universal inducer of the M-phase (Kishimoto, 2015).

MPF is the key regulator and driving force of M-phase transit. MPF regulates the changes in the cytoskeleton leading to the formation of the mitotic spindle, phosphorylates lamin to cause its depolymerization and consequently the nuclear envelope breakdown, and via the phosphorylation of histone H1 participates in chromosomes condensation (Nigg, 2001; Cukier, Li and Lee, 2007). Cyclin B is ubiquitinylated via APC/C and subsequently degraded in the proteasome in metaphase (Hagting *et al.*, 2002).

A representative schema of the cell cycle is depicted in the Figure 1.

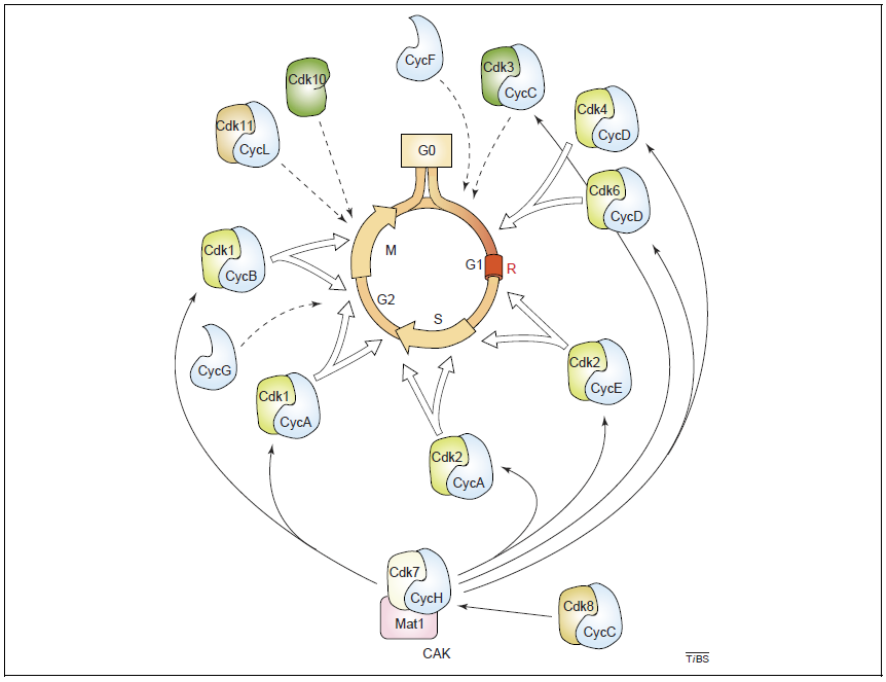

Figure 1 - Proposed roles of Cdk–cyclin complexes in the mammalian cell cycle.

Cdk4–CyclinD, Cdk6–CyclinD and Cdk3–CyclinC (at least in human cells) complexes regulate the G0–G1 transition (in quiescent cells) and the early phases of G1 (in proliferating cells) by phosphorylating the retinoblastoma protein (pRb). Cdk2–CyclinE complexes have been proposed to complete phosphorylation of pRb, an event that is thought to convey mitogenic independence (passage through the restriction point, R) to dividing cells. Cdk2–CyclinE complexes have been also implicated in the G1–S transition by licensing DNA origins of replication. Cdk2 later associates with Cyclin A during progression through S phase. Cdk1 participates in the S–G2 and G2–M transitions by sequential binding to Cyclin A and Cyclin B. These widely accepted roles for the Cdks are indicated by open arrows. Cdk-activating kinase (CAK) phosphorylates, and presumably activates, all cell-cycle Cdks. CAK, a protein complex formed of Cdk7, CyclinH and Mat1, is a substrate for Cdk8–CyclinC (filled arrows). Cdk10 and Cdk11 might be involved in mitosis, but their functional relevance is not well understood. Finally, Cyclin F might be required for entry into G1 and Cyclin G is implicated in the DNA damage response during the G2–M transition (see text). The functions of Cdk3, Cdk10, Cdk11, Cyclin F and Cyclin G are represented by dotted arrows to indicate that the data that implicate them in the cell cycle are still preliminary. (Figure and text from Malumbres & Barbacid 2005)

1.2 The cell cycle analysis

A cell population, regardless of whether represented by cells in a tissue culture, developmentally and immunophenotypically defined or differentiated cells in a tissue of a multicellular organism, is characterized by a unique and reproducible distribution of cells in the particular cell cycle phases under homeostatic conditions. Any disturbances in such cell populations caused by external factors (i.e. cell death, tissue injuries, synchronization in cell cycle etc.) result in changes in the distribution of cells in the various cell cycle phases. Cell cycle analysis is therefore a significant and widely used approach in deciphering the effect or mechanism of an external intervention or disease.

1.2.1 The S-phase cell determination

The S-phase represents the phase of DNA replication. This intricate process is strictly regulated and determines how many cells actively prepare for cell division. Several relatively feasible methods enable the determination of the proportion of cells in the S-phase in the whole population. Therefore, determining the fraction of cells actively synthesizing DNA has become a basic parameter in studies on the control and regulation of the cell cycle and cell and tissue responses to various stimuli.

Following the discovery of Howard and Pelc (1953) that DNA synthesis is restrained to a specific period of the cell life during its interphase between mitotic divisions, the incorporation of the radioactively labelled DNA precursor thymidine was widely used to determine cells engaged in DNA synthesis. It was further shown that the DNA synthesis period is separated from the mitotic divisions by two gaps, the G1-phase preceding thymidine incorporation, and the premitotic G2-phase after completing thymidine incorporation. Later on, the incorporation of halogenated thymidine precursors such as the commonly used analogue BrdU (5-bromo-2´-deoxy-uridine) became widely used to detect and measure cells in the S-phase. To determine the fraction of cells synthesizing DNA, BrdU is administered to cells *in vitro* or *in vivo* for a short period (usually 30-45 minutes) in order to incorporate a sufficient amount of BrdU into the DNA. Specific fluorescently labelled antibodies against BrdU then enable the visualization of BrdU positive cells (i.e. cells synthesizing DNA during exposure to the BrdU pulse) by microscopy or flow cytometry (Gonchoroff *et al.*, 1985, 1986; Takagi *et al.*,

1993).

The advantage of multicolour flow cytometry is the possibility to detect multiple fluorochromes and thus more antigenic structures in parallel. This approach enables us to also determine and quantify the proliferation in different cell subsets simultaneously, i.e. in the immunophenotypically defined cell subpopulations. In addition, DNA can be stained by intercalating fluorescent dyes, such as PI (propidium iodide), 7AAD (7-aminoactinomycin) and/or others which reveal the amount of DNA present in a particular cell. Combining BrdU labelling with total DNA staining can discriminate the actual cell distribution within the cell cycle (i.e. to discriminate G0/G1 phase, S-phase, G2/M phase) (Figure 2) (Ivanovska *et al.*, 2008; Kang *et al.*, 2013; Oguro, Ding and Morrison, 2013; Welschinger and Bendall, 2015). Another approach to the use of BrdU incorporation is based on its long-term *in vivo* application (repeated i.p., i.v. injections of BrdU solution or drinking BrdU supplemented water), which ensures the BrdU labelling of the majority of cells in tissues, including the slow-cycling cells. This can be followed by a chase phase without BrdU, lasting weeks to months, in which the labelled cells divide and BrdU incorporated in DNA is diluted with each cell division until it becomes undetectable. This approach, known as a long-term retaining assay, helps to identify the dormant and slow-cycling populations of stem and progenitor cells in various tissues (Wilson *et al.*, 2008; You *et al.*, 2011; Zhang *et al.*, 2015).

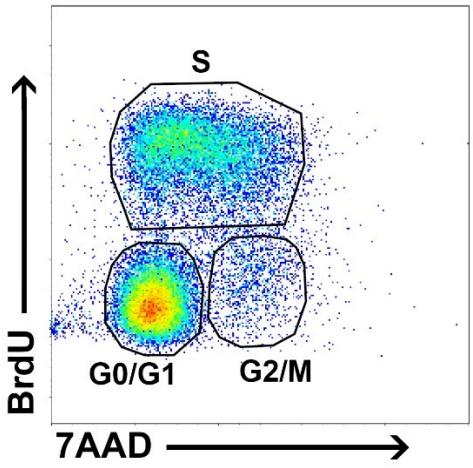

Figure 2 - Representative BrdU/7AAD dotplot of bone marrow cells.

1.2.2 Cell cycle flow rate measurement

The cumulative labelling protocol using BrdU, described by Nowakowski (1989) makes it possible, in addition to determining the proliferating cell fraction, to also establish the basic kinetic parameters of the cell cycle such as the duration of the S-phase, the duration of the cell cycle and the cell flow rate through the cell cycle. This protocol utilizes repeated *in vivo* applications of BrdU until all cycling cells are labelled with BrdU. The BrdU-labelled cells linearly increase during the BrdU labelling period. The durations of the S-phase and the cell cycle are then calculated from the slope of the increment in BrdU-labelled cells. However, this laborious approach is quite time consuming and requires many experimental animals when applied *in vivo*.

The availability of the two monoclonal antibodies against BrdU, 1) clone Br-3 specific only for BrdU and 2) clone IU-4 recognizing both BrdU and IdU (5-iodo-2´-deoxy-uridine, another thymidine analogue) enabled the development of a new method for sequential DNA labelling by two thymidine analogues for determining cell cycle kinetic parameters (Vanderlaan *et al.*, 1986; Shibui *et al.*, 1989). The experiments of Shibui (1989) aimed at an *in vitro* study of a human glioma cell line was based on the incubation of cells in the medium containing IdU and after a specific time interval **(T)** for a short time in the medium containing BrdU. The immunohistochemical analysis revealed three cell fractions: 1) the cells labelled only with IdU **(I+)**, 2) the cells double-labelled with IdU and BrdU **(I+B+)** and 3) unlabelled cells. **I+** cells exited the S-phase during time **T**. **I+B+** cells actively synthesizing DNA – the S-phase cell fraction. Unlabelled cells did not enter the S-phase during the labelling period (were in the G0-state or in G1-phase). Since **T** was known, the cell flow rate of cells into the G2-phase could be calculated as the **I+** cell fraction per **T**. The S-phase duration was then calculated according the equation: **(I+B+/I+) x T** and subsequently, assuming the expression of the cell fraction size in relative terms, the whole cell cycle length could be calculated as **T/I+**. Note that in order to avoid a false enrichment of the **I+** fraction caused by the division of these cells, the time interval **T** must not exceed the time required for passage through the G2- and M-phase.

This sophisticated dual thymidine analogues sequential DNA-labelling procedure greatly simplified the procedure for calculating the duration of the S-phase and the length of the cell cycle, and has been used in some *in vitro* and also *in vivo* studies (Ritter *et al.*, 1994; Pollack *et al.*, 1995; Raza *et al.*, 1997; Martynoga *et al.*, 2005; Yamada *et al.*, 2005).

This experimental approach for cell cycle analysis suffers from certain limitations. The labelling of DNA-synthesizing cells by the second thymidine analogue also takes a short but significant time, and as a result the cells leaving the S-phase and entering the G2-phase during this period are labelled with this thymidine analogue. The double-labelled population that should correspond to cells actively synthesizing DNA is thus slightly overestimated.

This slight inaccuracy can be solved by using another thymidine analogue, EdU (5-ethenyl-2´-deoxyuridine), which is incorporated into DNA during the S-phase similarly to halogenated thymidine analogues. In contrast to the halogenated thymidine analogues, EdU is detected through its reaction with fluorescent azides, in a Cu(I)-catalysed cycloaddition, instead by an antibody based detection (Salic and Mitchison, 2008). The availability of the mouse monoclonal antibody (clone MOBU-1) that specifically recognizes BrdU and does not cross-react with EdU allows these two thymidine analogues to be used in the dual EdU-BrdU labelling of cycling cells (Liboska *et al.*, 2012; Massey *et al.*, 2015). Because BrdU is preferentially incorporated into DNA in the presence of EdU (Bradford and Clarke, 2011), three labelled cell fractions can be distinguished: the EdU single labeled cells (**E+B-**), the EdU and BrdU double-labelled cells **(E+B+)** (in analogy to the IdU–BrdU labelling procedure mentioned above) and the BrdU single-labelled cells (**E-B+**). The **E-B+** cell fraction represents the cells which started DNA synthesis after BrdU administration until the bone marrow collection.

The principle of dual sequential DNA labelling with EdU and BrdU is depicted in Figure 3.

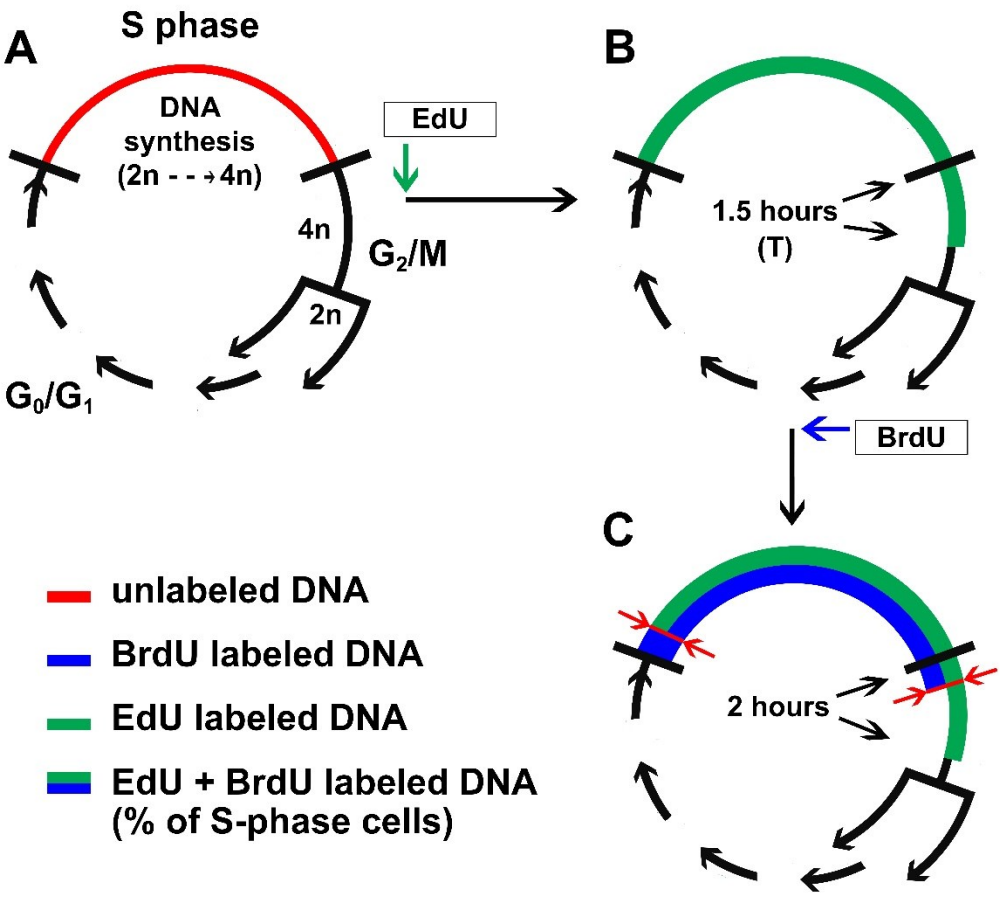

Figure 3 - EdU – BrdU dual labeling of DNA

A) *Cell cycle with highlighted S-phase (red)*

B) *EdU labels DNA (green) after its administration for period T (1.5 hrs) – all S-phase cells plus those that left the S-phase during T were labelled*

C) *Half an hour after BrdU administration, all S-phase cells were double-labelled with both EdU (green) and BrdU (blue). EdU-only labeled cells indicate the cells that left the S-phase during T. BrdU-only labeled cells (blue) represent cells entering the S-phase in the first half hour after BrdU administration.*

1.3 Haematopoietic stem and progenitor cells (HSPCs)

Haematopoiesis is a highly efficient cell-producing system with a hierarchical structure consisting of haematopoietic stem cells (HSCs) at the apex, progenitors in the middle and differentiated precursors of blood cells at the bottom.

The introduction of flow cytometry into experimental studies of haematopoietic tissue enabled the identification of various types of immature haematopoietic cells. In the adult mouse, the population highly enriched by HSCs and haematopoietic progenitors can be identified through the expression of surface antigens discernible by monoclonal antibodies. These immature haematopoietic cells lack expression of the markers characteristic for lineages of differentiated myeloid and lymphoid blood cells (Lineage markers: CD3, Gr-1, Mac-1, B220, Ter119) and conversely express Sca-1 (Stem cell antigen) and c-Kit tyrosine kinase receptor for the cytokine stem cell factor (CD117). These are often abbreviated Lin^- $Sca\text{-}1^+c\text{-}Kit^+$ or LSK cells (Spangrude, Heimfeld and Weissman, 1988; Okada *et al.*, 1991; Ikuta and Weissman, 1992) and represent the starting population for their further division into several populations of haematopoietic stem and progenitor cells (HSPCs) (Challen *et al.*, 2009). Additional markers such as Flt3 or SLAM (Signalling lymphocytic activation molecule) protein family CD48 and CD150 (Adolfsson *et al.*, 2001; Kiel *et al.*, 2005) and some others such as endoglins (CD105) (Chen *et al.*, 2002, 2003) are currently used for this purpose. The SLAM markers are the most frequently used to distinguish HSPCs with various specific developmental potentials. LSK cells are divided according to their CD150 and CD48 expression patterns to $CD150^+CD48^-$ haematopoietic stem cells (HSCs), $CD150^-CD48^-$ multipotent progenitors (MPPs), and two types of developmentally more restricted progenitors (HPCs-1 and HPCs-2) $CD150^-CD48^+$ and $CD150^+CD48^+$, respectively (Forsberg *et al.*, 2005; Kiel *et al.*, 2005; Weksberg *et al.*, 2008; Oguro, Ding and Morrison, 2013). Alternatively, HSCs can be identified by their high level of Hoechst33342 efflux activity, mediated by transmembrane ATP-binding cassette protein transporters (ABC transporters) (Goodell *et al.*, 1996; Zhou *et al.*, 2001), and particularly with their high expression level of CD150 (Savvulidi and Šefc, unpublished) or of CD105 (Chen *et al.*, 2002, 2003).

Whereas the LSK population contains the majority of primitive HSPCs, the loss of the Sca-1 antigen shifts this population to a more advanced progenitor pool. LS^-K cells lacking the

IL7 receptor represent developmentally advanced myeloid-committed progenitors that are restricted in their developmental potential to granulocytes, macrophages, megakaryocytes and erythroid cells. $LS^{-}K$ cells can be further divided according to the expression of CD34 and CD16_32 (FcγR III/II) to CMPs (common myeloid progenitors) $CD34^{+}CD16\_32^{-}$, GMPs (granulocyte-macrophage progenitors) $CD34^{+}CD16\_32^{+}$ and MEPs (megakaryocyte-erythroid progenitors) $CD34^{-}CD16\_32^{-}$ (Figure 5) (Akashi *et al.*, 2000; Na Nakorn *et al.*, 2002). The lymphoid-biased progenitor population downstream of LSK are common lymphoid progenitors (CLPs) $LS^{int.}K^{int.}IL7R^{+}$ (Kondo, Weissman and Akashi, 1997).

1.4 Dual EdU-BrdU sequential DNA-labelling technique in the study of haematopoiesis

Two papers have recently been published that explore cell cycle kinetics in the differentiating adult or foetal haematopoietic tissue (Hwang *et al.*, 2017; Akinduro *et al.*, 2018). In both studies, the dual sequential DNA-labelling technique with EdU and BrdU was used *in vivo*. The study published by Akinduro et al. (2018) compared the proliferation dynamics of myeloid leukemia progenitors and normal haematopoietic progenitors. The dual sequential DNA-labelling technique used a single EdU dose followed by a single BrdU dose after the time interval **T**. The flow rate of the cells entering into the S-phase, the **E-B+** cell fraction within **T**, was determined. This approach supposed a limited bioavailability of EdU *in vivo*, approximately 0.5 hour (assumed e.g. by Akinduro et al. 2018). It is important to emphasize that when there is limited EdU bioavailability, the dual labelled **E+B+** fraction is underestimated. This would disqualify this experimental setting for determining the duration of the S-phase. However, the approach would be adequate for determining the cell cycle flow rate as applied by Akiduro et al. (2018). Obviously, the low frequency and very low proliferation rate of HSCs and multipotent progenitors in undisturbed murine haematopoiesis (LSK $CD48^{-}$ cells) causes the data for these cells to be calculated from a very low cell number and thus they are less precise than in $CD48^{+}$ progenitor cells.

The second study published by Hwang et al. (2017) demonstrates the shortening of the S-phase in two consecutive developmental stages of the foetal erythroid progenitors. Hwang also used the dual sequential DNA-labelling technique with a single EdU dose followed by a

single BrdU dose separated by **T**. In contrast to the Akinduro et al. (2018), the fractions of **E+B-** (i.e. cells leaving the S-phase) and all BrdU-positive (**E+B+** + **E-B+**) cells were used for calculating the duration of the cell cycle and cell cycle phases. The BrdU pulse was maximally truncated so the enrichment of the S-phase fraction by the cells that had started new DNA synthesis during this BrdU pulse was negligible, therefore all BrdU-positive cells were considered to be S-phase cells. However, the calculated G2/M duration of the erythroid progenitors, designated CFU-E (colony-forming units-erythrocyte), is shorter than **T**. This small discrepancy between the calculated G2/M phase duration and the chosen **T** highly suggests the false enrichment of the **E+B-** fraction by cells that have doubled by the mitotic division and that therefore the chosen **T** for exploring the cell cycle kinetics of CFU-E by the EdU-BrdU technique was too long.

The dual sequential DNA-labelling technique with EdU and BrdU for *in vivo* use represents a sophisticated and powerful technique for studying cell cycle kinetics, but as discussed above, it requires a very precise execution and caution in data interpretation.

1.5 The cell cycle activity of haematopoietic stem and progenitor cells

HSCs represent a heterogeneous population of multipotent cells (Morita, Ema and Nakauchi, 2010; Sanjuan-Pla *et al.*, 2013; Carrelha *et al.*, 2018) located in the bone marrow. HSCs through symmetric (producing two HSCs or two progenitors) or asymmetric (producing one HSCs and one progenitor) divisions replenish the pool of lineage-committed progenitors which multiply and differentiate into mature blood cells. HSCs also maintain their own population (self-renewal) over the lifetime of the organism.

Two label-retaining assay studies, using BrdU or the transient expression of a Histone2B (H2B)-Green Fluorescent Protein (GFP) fusion protein, followed by computational modelling of the label dilution kinetics in HSCs, revealed two fractions of HSCs, the dormant HSCs (d-HSCs) and active HSCs (a-HSCs). The results from this mathematical modelling suggested that d-HSCs (representing 15% of the HSC population) and a-HSCs (representing 85% of the HSC population) divide approximately once every 145 days and once every 36 days respectively (Wilson *et al.*, 2008; Foudi *et al.*, 2009). Moreover, the competitive reconstitution experiments found that the d-HSCs in contrast to a-HSCs possess the vast majority of the

multilineage long-term self-renewing cells (Wilson *et al.*, 2008; Foudi *et al.*, 2009). The capacity for self-renewing cell divisions, either asymmetric or symmetric, had been thought to be a specific feature of HSCs that is lost with their differentiation. Interestingly, Qiu et al. (2014) published a paper suggesting that once a dormant HSC started to proliferate, it was destined for clonal extinction. Conceptually, this finding is in contradiction with the results which demonstrated the capacity of single transplanted HSCs to establish the entire haematopoiesis over the long term, capable of transplantation to secondary and tertiary myeloablated recipients (Morita, Ema and Nakauchi, 2010). The experiments with single-cell transplantation thus convincingly demonstrate the capacity of HSCs to proliferate, replenish their own population and support the production of blood cells in the long term. They also correspond to the idea that HSCs can switch between the a-HSC and d-HSC states of proliferation (Wilson *et al.*, 2008).

To maintain the correct balance between self-renewal and differentiation, HSCs reside in specialized microenvironments in the bone marrow called niches. The concept of the stem cell niche developed as new experimental results became available. It was recently found that stem cell niches for dividing and non-dividing HSCs are formed by perivascular leptin-positive stromal cells localized around sinusoids in the murine bone marrow. These cells express the cytokines stem cell factor (SCF) and Cxcl12 (SDF-1) (Zhou *et al.*, 2014; Acar *et al.*, 2015). The cell cycle analysis using short-term BrdU incorporation and Hoechst33342 staining showed an immense range of proliferation rates existing in various types of HSPCs (Passegué *et al.*, 2005; Foudi *et al.*, 2009; Oguro, Ding and Morrison, 2013). Collectively, these results suggest a proliferation hierarchy in HSPCs corresponding to their developmental hierarchy, in which the cells increase their proliferation rate concomitantly with their advancing differentiation.

1.6 Quantification of murine haematopoiesis

Intensive cell proliferation resulting in the production of mature blood cells over the whole lifespan is a characteristic feature of haematopoietic tissue. In mice, approximately 300 million bone marrow cells generate 200-250 million of various types of myeloid blood cells every day (Novak and Necas, 1994; Necas *et al.*, 1995). This sustained production of blood cells is traditionally viewed as being derived from a miniscule supply of multipotent cells generated

by the asymmetric division of HSCs. Approximately 25 000 – 50 000 HSCs, immunophenotyped as LSK CD150+/48-, are found in mouse bone marrow (Nakada *et al.*, 2014). Assuming that only 15% of this HSC population are d-HSCs (i.e. "true" haematopoietic stem cells with long-term repopulating potential) (Wilson *et al.*, 2008), then the enormous blood cell production begins with only approximately 4000 – 8000 HSCs. This number corresponds to another independent estimate made by Forgacova et al. (2013).

Busch et al. (2015) prepared a knock-in mutant mouse that enabled the inducible genetic labelling of most primitive HSCs. The yellow fluorescent protein (YFP) expression was driven from the Tie2 locus, which is expressed in most primitive HSCs (Yano *et al.*, 1997; Arai *et al.*, 2004). This approach thus enabled the induction of YFP production in HSCs and measurement of the cell label progression downstream in the haematopoietic compartments over time. The results revealed only a miniscule input of HSCs into their downstream descendent MPPs. Hence, the MPPs and the restricted progenitors (LSK CD150-/CD48+) were the major source for differentiated blood cell lineages in steady-state haematopoiesis. This is consistent with the results and conclusions of Akinduro et al. (2018), who also identified the restricted progenitors (LSK CD150-/CD48+) as the main contributors of cell production within the LSK population of immature haematopoietic cells.

1.7 Erythropoiesis

1.7.1 Embryonal erythropoiesis

Embryonal haematopoiesis occurs in three waves. The first wave, which is almost purely erythropoietic in nature and known as the primitive erythropoiesis, originates from unique erythropoietic progenitor cells, EryP-CFC (primitive erythroid colony-forming cells) detectable on the embryonic day 7.25 (E7.25) in the yolk sac. EryP-CFCs form clusters of primitive erythroblasts surrounded by endothelial cells, the “blood islands”, and their numbers peak at E8.5. Around E9 EryP-CFCs enter into the circulation as large nucleated cells to differentiate in the blood into mature enucleated red blood cells between E9-E12.5. This primitive wave of erythropoiesis is only transient, as EryP-CFCs are no longer detectable in the yolk sac after E9.

The second and third waves of embryonal haematopoiesis are collectively referred to as the definitive haematopoiesis that gives rise to all blood cell lineages. The initiation of haematopoietic differentiation taking place in the foetal liver is a common feature of these two waves, but they differ in the place of origin. While the second wave is derived from the erythromyeloid precursors detected in the yolk sac at E8.5 which, within 48 hours, expand and via circulation colonize the foetal liver, the third wave arises from HSCs originally generated in the aorta gonad mesonephros region (AGM) at E10.5-E11.5 and in the placenta at E10.5-E13. These HSCs also subsequently colonize the foetal liver. HSCs extensively proliferate and thus amplify their numbers in the foetal liver and are further spread during prenatal development into other haematopoietic organs (the spleen, bone marrow, thymus). In contrast to primitive erythropoiesis, the erythroid differentiation derived from HSCs occurs exclusively extravascularly (Figure 4) (Baron, Isern and Fraser, 2012; Baron, 2013; Palis, 2014; Udroiu, 2016)

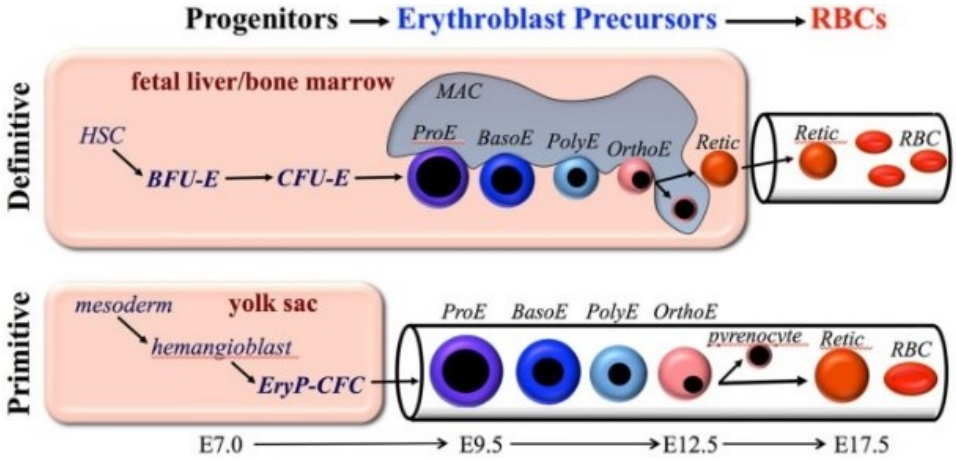

Figure 4 - Overview of primitive and definitive eythropoiesis

Both forms of erythroid cell production are characterized by the progressive movement of cells through three compartments: progenitors, erythroblast precursors, and red blood cells (RBCs). Erythroid progenitors (BFU-E, CFU-E, and EryP-CFC) are defined by their capacity to form colonies of maturing erythroid cells in vitro. Erythroid precursors are defined morphologically as proerythroblasts (ProE), basophilic erythroblasts (BasoE), polychromatophilic erythroblasts (PolyE), and orthochromatic erythroblasts (OrthoE). OrthoE enucleate to form a pyrenocyte, that contains the condensed nucleus, and a reticulocyte (Retic), that goes on to mature in to a RBC. Definitive erythropoiesis in the adult organism is derived from hematopoietic stem cells (HSC), while primitive erythropoiesis occurs just once from mesoderm cells in the early embryo. (Figure and text from Palis, 2014)

1.7.2 Adult erythropoiesis

The postnatal development of red blood cells takes place in the bone marrow. The differentiation of HSCs to early lineage-committed progenitors is driven by a random fluctuation of lineage-specific transcription factors together with the action of cytokines produced by the bone marrow microenvironment (Orkin, 2000; Metcalf, 2008; Mossadegh-Keller *et al.*, 2013; Grover *et al.*, 2014). The transcription regulators PU.1 and GATA-1, and their mutual interaction, play a crucial role in the initiation of erythroid differentiation. While MPPs expressing transcription factor PU.1 induce myeloid and lymphoid lineage commitment, MPPs expressing GATA-1 display myelo-erythroid potential (Nerlov and Graf, 1998; Arinobu

et al., 2007). There is a mutual inhibitory relationship between these two transcription factors and therefore the random overexpression of one of these transcription factors leads to the repression of the other one and thus determines the lineage decision of MPPs (Nerlov *et al.*, 2000; Zhang *et al.*, 2000; Cantor and Orkin, 2001). However, this accepted mechanism of lineage commitment based on the PU.1 to GATA-1 interaction as the driving factor of MPP lineage decision has been recently challenged by the study of Hoppe et al. suggesting that these interactions serve as a reinforcement but not the cell fate decision mechanism in MPPs (Hoppe *et al.*, 2016).

Once the erythroid differentiation program is induced, MPPs give rise to CMPs and subsequently to MEPs, followed by two progenitors stages, traditionally identified via *in vitro* cultivation in semisolid medium, burst-forming units-erythroid (BFU-E) and colony-forming unit-erythroid (CFU-E) (Stephenson *et al.*, 1971; McLeod, Shreeve and Axelrad, 1974; Gregory and Eaves, 1978). While several factors (stem cell factor (SCF), interleukin-3 (IL-3), insulin-like growth factor 1 (IGF-1), granulocyte-macrophage colony-stimulating factor (GM-CSF), and erythropoietin (Epo) are involved in the control of BFU-E cells, CFU-E cells are highly dependent on Epo, which is necessary for their survival, proliferation and further differentiation (Kannourakis and Johnson, 1988; Dai, Krantz and Zsebo, 1991; Muta *et al.*, 1994; Lewis *et al.*, 1998; Elliott, Pham and Macdougall, 2008).

The terminal erythroid differentiation occurs in erythroblastic islands in bone marrow where proerythroblasts, the descendant of CFU-E cells, mature through the stages of basophilic, polychromatic to the orthochromatic erythroblasts that undergo enucleation, a process of nucleus removing, thus giving rise to the reticulocytes. Reticulocytes further autophagically remove organelles and extensively remodel their membrane to finally transform into erythrocytes. The erythroblastic islands consists of a central macrophage surrounded by maturing erythroblasts. The central macrophage interacts with erythroblasts through surface-adhesive molecules, supports erythroblasts with iron, produces cytokines and phagocytes the nuclei (Dzierzak and Philipsen, 2013; Moras, Lefevre and Ostuni, 2017).

1.7.3 Identification of erythroid progenitors and precursors

Thorough studies on the changes in the expression of surface antigens occurring during the early and terminal phases of erythropoiesis have allowed the immunophenotypic identification of individual erythroid progenitors by flow cytometry. From this point of view, the most often used markers are Ter119, transferrin receptor (CD71) and CD44. The Ter119 antigen is associated with glycophorin A and is detectable from the proerythroblastic stage to mature erythrocytes (Kina *et al.*, 2000). CD71 expression is initiated during the progenitor CFU-E stage, further enhanced upon the induction of hemoglobinization (i.e. in stages of proerythroblasts and erythroblasts), decreases in the reticulocyte stage and is lost in mature erythrocytes (Lok and Ponka, 2000; Pop *et al.*, 2010). Therefore, the expression pattern of CD71/Ter119 corresponds well to the maturation stages of proerythroblasts and erythroblasts during the terminal phase of erythropoiesis (Koulnis *et al.*, 2011).

The CD44 surface antigen involved in cell-to-cell or cell-to-extracellular matrix interactions is highly expressed in proerythroblasts. CD44 expression dramatically decreases from the proerythroblast stage to the reticulocyte stage. The immunophenotypic identification of erythroid progenitors based on their CD44/Ter119 expression pattern (Chen *et al.*, 2009) is thus an alternative to the more frequently used CD71/Ter119 expression pattern.

Imaging flow cytometry combines flow cytometry with fluorescent microscopy and thus allows a direct correlation of antigenic and other cell markers with basic cell morphology. This enables a further refinement of the characterization of developing erythroid cells (McGrath, Bushnell and Palis, 2008; Mcgrath, Catherman and Palis, 2017).

1.7.4 S-phase specific erythroid differentiation

Erythropoiesis is a process in which immature erythropoietic progenitors and precursors intensively proliferate and simultaneously differentiate to generate a sufficient number of fully matured red blood cells. However, the interrelation between cell cycle and differentiation remains poorly understood.

The study published by Pop et al. (2010) exploring erythropoiesis in the foetal liver identified an unique link between the cell cycle and the early phase of erythroid differentiation. They found that the $Ter119^{-}CD71^{-/low}$ cells corresponding to CFU-E erythroid progenitors intensively express the CD71 antigen and expose it on their cell surface during the S-phase in the final cell cycle of this progenitor stage. This augmentation of CD71 expression is thus tightly linked to the S-phase, which suggests a direct mechanistic link between cell cycle progression and cell differentiation. This differentiation step in the late CFU-E cell stage occurs within the S-phase of a single cell cycle and, besides the augmented CD71 expression, also involves the onset of the Ter119 expression which transforms CFU-E cells into proerythroblasts.

CFU-E cells require stimulation with Epo that is essential for their survival and proliferation, and also drives their differentiation (Wu *et al.*, 1995). The signalling pathway activated by Epo results in GATA-1 phosphorylation. GATA-1 is the erythroid-specific transcription factor which is upregulated in CFU-E cells. GATA-1 can form a complex with pRb/E2F-2 and thus participate in an inhibition of proliferation (Kadri *et al.*, 2009). Once phosphorylated, GATA-1 is able to associate with friend-of-GATA-1 protein (FOG-1) that serves as a cofactor for GATA-1 in the control of the genes crucial for erythropoiesis. GATA-1 phosphorylation and its association with FOG-1 also leads to the displacement of E2F-2 from the pRb/E2F-2 complex and the released E2F-2 triggers cell proliferation (Tsang *et al.*, 1997; Kadri *et al.*, 2015).

The other crucial event occurring specifically in late CFU-E cells is down-regulation of the cyclin-dependent kinase inhibitor $p57^{KIP2}$. $p57^{KIP2}$ downregulation leads to an increase in the replication fork speed and to a shortening of the S-phase in this specific final cell cycle of CFU-E progenitor cells (Hwang *et al.*, 2017).

2 Hypothesis

The sustained production of blood cells is the principal function of haematopoietic tissue. Blood cell production results from the intensive proliferation of haematopoietic cells. In mice, approximately 300 million bone marrow cells generate 200-250 million of various types of myeloid blood cells every day. The sustained production of blood cells is traditionally viewed as being derived from a miniscule supply of haematopoietic stem cells (HSCs). These stem cells possess self-renewal capacity or can differentiate into progenitor cells that further proliferate and differentiate into mature blood cells.

We hypothesize that self-renewing capacity is not confined to stem cells in the developmental hierarchy of haematopoietic stem and progenitor cells (HSPCs). We expect that an in-depth analysis of the cell cycle characteristics of HSPCs would provide novel information regarding the self-renewing capability of HSPCs.

The formation of red blood cells represents a significant part of haematopoiesis. In foetal liver haematopoiesis, the development of early erythroid cells has been reported to occur in the S-phase of the cell cycle.

We hypothesize that cell proliferation and differentiation are also closely linked during erythroid development in adult bone marrow. We expect that a thorough analysis of the cell cycle in early erythroid progenitors would uncover the relationship between the cell cycle and differentiation.

Aims of the study

1. **To determine the proliferating rate in immunophenotypically defined populations of HSPCs and to compare it to their corresponding developmental hierarchy.**

2. **To introduce and optimize the dual thymidine analogue sequential DNA-labelling technique *in vivo* for the analysis of the proliferation and differentiation of HSPCs.**

3. **To semi-quantify the cell production arising from different haematopoietic subpopulations by determining the cell cycle parameters in various HSPCs.**

4. **To determine the interrelationship between the proliferation and differentiation of early erythropoietic progenitor cells by using the dual thymidine analogue sequential DNA-labelling technique**

3 Materials and Methods

3.1 Materials

3.1.1 Chemicals

7-AAD (7-aminoactomycin D) (*BD Biosciences, USA*)

APC BrdU Flow Kit (*BD Biosciences, USA)*

Bovine serum albumin – Fraction V, biotin free (*Carl Roth GmbH*, *Germany*)

BrdU (5-bromo-2´-deoxyuridine) (*Sigma-Aldrich, USA*)

Click-iT^{TM} Plus EdU Alexa Fluor 488 Flow Cytometry Assay Kit (*ThermoFisher Scientific, USA)*

Colchicine (*Sigma-Aldrich, USA*)

CS&T beads (*BD Biosciences, USA*)

Disodium phosphate ($Na_2HPO_4.12H_2O$) (*IPL, Czech Republic*)

EdU (5-ethynyl-2´-deoxyuridine) (*ThermoFisher Scientific, USA*)

IMDM (Iscove's Modified Dulbecco's Medium) (*Sigma-Aldrich, USA*)

Methocult^{TM} SF M3436 (Serum-free methylcellulose-based medium with recombinant cytokines (including EPO) for mouse erythroid progenitor cells) (STEMCELL Technologies Inc., Canada)

Methocult^{TM} M3436 (Methylcellulose-based medium with EPO (without other cytokines) for mouse cells) (STEMCELL Technologies Inc., Canada)

Monosodium phosphate ($NaH_2PO_4.2H_2O$) (*IPL, Czech Republic*)

Sodium chloride (NaCl) (*IPL, Czech Republic*)

Türck solution (*Penta, Czech Republic)*

3.1.2 Antibodies

1) Immature haematopoietic cells

"LSK SLAM, CMPs, GMPs, MEPs" panel

Alexa Fluor 700-conjugated lineage antibody cocktail (*BioLegend, USA*)

APC-conjugated anti-mouse CD48 (*BioLegend, USA*)

Biotin-conjugated anti-mouse CD34 (*eBioscience, USA*)

Brilliant Violet 421-conjugated anti-mouse CD117 (c-Kit) (*BioLegend, USA*)

Brilliant Violet 510-conjugated anti-mouse CD16_32 (FcγRIII/II) (*BioLegend, USA*)

Brilliant Violet 605-conjugated anti-mouse CD150 (*BioLegend, USA*)

Brilliant Violet 785-conjugated anti-mouse CD127 (IL-7Rα) (*BioLegend, USA*)

PE-conjugated anti-mouse Ly-6A/E (Sca-1) (*BioLegend, USA*)

PECy7-conjugated streptavidin (*BioLegend, USA*)

"Cell cycle" panel for LSK SLAM

7AAD (DNA labelling) (*BD Biosciences, USA*)

APC-conjugated anti-BrdU (*BD Biosciences, USA*)

Brilliant Violet 421-conjugated anti-mouse CD117 (c-Kit) (*BioLegend, USA*)

Brilliant Violet 605-conjugated anti-mouse CD150 (*BioLegend, USA*)

FITC-conjugated lineage antibody cocktail (*BioLegend, USA*)

PE-conjugated anti-mouse Ly-6A/E (Sca-1) (*BioLegend, USA*)

PECy7-conjugated anti-mouse CD48 (*BioLegend, USA*)

"Cell cycle" panel for CMPs, GMPs, MEPs

7AAD (DNA labelling) (*BD Biosciences, USA*)

APC-conjugated anti-BrdU (*BD Biosciences, USA*)

Biotin-conjugated anti-mouse CD34 (*eBioscience, USA*)

Brilliant Violet 421-conjugated anti-mouse CD117 (c-Kit) (*BioLegend, USA*)

Brilliant Violet 510-conjugated anti-mouse CD16_32 (FcγRIII/II) (*BioLegend, USA*)

Brilliant Violet 785-conjugated anti-mouse CD127 (IL-7Rα) (*BioLegend, USA*)

FITC-conjugated lineage antibody cocktail (*BioLegend, USA*)

PE-conjugated anti-mouse Ly-6A/E (Sca-1) (*BioLegend, USA*)

PE/Cy7-conjugated streptavidin (*BioLegend, USA*)

"Cell cycle flow rate" panel for LSK cells, CMPs, GMPs, MEPs

Alexa Fluor 488 azide detecting Edu by Click-iT® reaction (*ThermoFisher Scientific, USA*)

Alexa Fluor 700-conjugated lineage antibody cocktail (*BioLegend, USA*)

APC-conjugated anti-mouse CD16_32 (FcγRIII/II) (*BioLegend, USA*)

APC/Cy7-conjugated streptavidin (*BioLegend, USA*)

Biotin-conjugated anti-mouse CD34 (*eBioscience, USA*)

Brilliant Violet 785-conjugated anti-mouse CD127 (IL-7Rα) (*BioLegend, USA*)

Pacific Blue-conjugated anti-BrdU (*ThermoFisher Scientific, USA*)

PE-conjugated anti-mouse CD117 (c-Kit) (*BioLegend, USA*)

PE/Cy7-conjugated anti-mouse Ly-6A/E (Sca-1) (*BioLegend, USA*)

2) Erythroid progenitor and precursor cells

"Erythroid differentiation" panel

APC/Cy7-conjugated anti-mouse Ly-6G/Ly6C (Gr-1) (*Sony Biotechnology, USA*)

APC/Fire™ 750-conjugated anti-mouse CD11b (Mac-1) (*BioLegend, USA*)

APC/Fire™ 750-conjugated anti-mouse CD45R/B220 (*BioLegend, USA*)

APC-conjugated anti-mouse Ly-6A/E (Sca-1) (*BioLegend, USA*)

Brilliant Violet 421-conjugated anti-mouse CD117 (c-Kit) (*BioLegend, USA*)

Brilliant Violet 510-conjugated anti-mouse CD16_32 (FcγRIII/II) (*BioLegend, USA*)

Brilliant Violet 785-conjugated anti-mouse Ter119 (*BioLegend, USA*)

PE-conjugated anti-mouse CD71 (*BioLegend, USA*)

"Cell cycle" panel

7AAD (DNA labelling) (*BD Biosciences, USA*)

APC/Cy7-conjugated anti-mouse Ly-6G/Ly6C (Gr-1) (*Sony Biotechnology, USA*)

APC/Fire ™ 750-conjugated anti-mouse CD11b (Mac-1) (*BioLegend, USA*)

APC/Fire ™ 750-conjugated anti-mouse CD45R/B220 (*BioLegend, USA*)

APC-conjugated anti-mouse CD16_32 (FcγRIII/II) (*BioLegend, USA*)

Biotin-conjugated anti-mouse CD117 (c-Kit) (BioLegend*, USA*)

Brilliant Violet 605-conjugated streptavidin (*BioLegend, USA*)

Brilliant Violet 785-conjugated anti-mouse Ter119 (*BioLegend, USA*)

Pacific Blue-conjugated anti-BrdU (*ThermoFisher Scientific, USA*)

PE-conjugated anti-mouse CD71 (*BioLegend, USA*)

PE/Cy7-conjugated anti-mouse Ly-6A/E (Sca-1) (*BioLegend, USA*)

"Cell cycle flow rate" panel

7AAD (DNA labelling) (*BD Biosciences, USA*)

Alexa Fluor 488 azide detecting Edu by Click-iT® reaction (*ThermoFisher Scientific, USA*)

APC/Cy7-conjugated anti-mouse Ly-6G/Ly6C (Gr-1) (*Sony Biotechnology, USA*)

APC/Fire™ 750-conjugated anti-mouse CD11b (Mac-1) (*BioLegend, USA*)

APC/Fire™ 750-conjugated anti-mouse CD45R/B220 (*BioLegend, USA*)

APC-conjugated anti-mouse CD16_32 (FcγRIII/II) (*BioLegend, USA*)

Biotin-conjugated anti-mouse CD117 (c-Kit) (BioLegend*, USA*)

Brilliant Violet 605-conjugated streptavidin (*BioLegend, USA*)

Brilliant Violet 785-conjugated anti-mouse Ter119 (*BioLegend, USA*)

Pacific Blue-conjugated anti-BrdU (*ThermoFisher Scientific, USA*)

PE-conjugated anti-mouse CD71 (*BioLegend, USA*)

PE/Cy7-conjugated anti-mouse Ly-6A/E (Sca-1) (*BioLegend, USA*)

3.1.3 Buffers

Phosphate buffered saline (PBS): 16 mmol/l $Na_2HPO_4.12H_2O$, 4mmol/l $NaH_2PO_4.2H_2O$, 0.15 mol/l NaCl, pH 7.4

3.2 Instruments and software

Instruments

AccuBlock™ Digital Dry Bath (*Labnet International, USA*)

Analytical balance AB104 (*Mettler Toledo, Czech Republic*)

Automatic micropipetes (*Eppendorf, Germany*)

Cellometer AUTO T4 (*Nexcelom Bioscience, USA*)

Centrifuge 5415D (*Eppendorf, Germany*)

Centrifuge 5415R (*Eppendorf, Germany*)

Centrifuge 5804R (*Eppendorf, Germany*)

$C0_2$ incubator HERAcell 150 (*Heraeus, Germany*)

Flow box Holten LaminAir, Model 1.2 (*Thermo-Scientific Inc., USA*)

Flow cytometers: 1) FACS Canto II flow cytometer, equipped with 405 nm (60 mW), 488 nm (20 mW) and 633 nm (15 mW) lasers (*BD Biosciences, USA*)

2) FACSAria IIu cell sorter equipped with 489 nm (50 mW), 561 nm (100 mW), 638 nm (140 mW), 404 nm (100 Mw) and 355 nm (20 mW) lasers (*BD Biosciences, USA*)

Imaging flow cytometer: AMNIS ImageStream X Mark II cytometer, equipped with 375 nm, 405 nm, 488 nm, 561 nm, 642 nm and 785 nm lasers under 40x software magnification, (*Amnis-EMD Millipore, USA*)

Reusable Laboratory Micro Array Slide Spinner (*Labnet International, USA*)

Wizard IR Vortex Mixer (*Velp Scientifica, Italy*)

Software

BD FACSDiva software version 6.1.3 (*BD Biosciences, USA*)

FlowJo vX software (*Tree Star Inc., USA*)

IDEAS analysis software (v.6.1) (*Amnis-EMD Millipore, USA*)

INSPIRE system software (part number: 780-01286-01, Rev. B) (*Amnis-EMD Millipore, USA*)

3.3 Experimental animals

Male and female C57BL/6J mice 6-12 weeks of age were used. Mice were bred in the specific pathogen-free facility of the Center of Experimental Biomodels, First Faculty of Medicine, Charles University. The experiments were approved by the Laboratory Animal Care and Use Committee of the First Faculty of Medicine, Charles University; and the Ministry of Education, Youth and Sports of the Czech Republic (MSMT-6316/2014-46).

3.4 Bone marrow collection

Bone marrow was flushed from femurs of mice sacrificed by cervical dislocation with ice-cold solution of 1% bovine serum albumin in phosphate-buffered saline (PBS/BSA) prepared in the laboratory. Cell concentration was measured with a Cellometer^{TM} Auto T4 automated cell counter, using Türck solution for white blood cell count.

3.5 Immunophenotyping of cell populations

Bone marrow cells (BMCs) (4 x 10^6 cells) were pelleted by centrifugation (400 g, 5 min, 4 °C) and cells in the pellet were incubated with a corresponding combination of fluorochrome-conjugated antibodies on ice for 30 min in the dark. Cells were then washed by PBS/BSA and resuspended in 250 µl of PBS/BSA.

To identify HSPCs according to Kiel et al. (2005) and Oguro et al. (2013) and the myeloid progenitors according to Akashi et al. (2000), the BMCs were stained against lineage markers (CD45R/B220, CD3, Ly-6G/Ly6C (Gr-1), CD11b (Mac-1), Ter119) (2.5 µl per sample) for exclusion of progenitors in a terminal phase of their differentiation, and markers for distinguishing immature haematopoietic cells (Ly6A/E (Sca-1), CD117 (c-Kit), CD48, CD150, CD127 (IL-7Rα), CD16_32 (FcγRIII/II), CD34) (1 µl of each antibody per sample). The gating strategy is shown on the Figure 5.

To identify erythroid progenitor and precursor cells, the BMCs were stained against lineage markers (CD45R/B220, Ly-6G/Ly6C (Gr-1), CD11b (Mac-1)) (2.5 µl per sample) to exclude granulopoietic and lymphopoietic progenitors in a terminal phase of their differentiation, CD16_32 (FcγRIII/II) (1 µl per sample) to exclude early granulopoietic progenitors,

Ly6A/E (Sca-1) (1 µl per sample) to exclude immature haematopoietic cells and markers for distinguishing the erythroid progenitor and precursor cells in various phases of their differentiation (CD117 (c-Kit), CD71, Ter119) (1 µl of each antibody per sample). The gating strategy is shown on the Figure 15A.

3.6 Cell cycle analysis

3.6.1 Percentage of DNA-synthesizing cells determined by *in vitro* staining

An APC BrdU Flow kit was used to determine the percentage of various types of HSPCs and myeloid progenitors engaged in DNA synthesis, i.e. in the S-phase of the cell cycle. Four millions of bone marrow cells were incubated for 45 min *in vitro* in 2 ml IMDM medium containing 10 µM BrdU (5-bromo-2´-deoxyuridine) (37°C, 5% CO_2 atmosphere). The whole procedure was performed according to the APC BrdU Flow kit instructions. Briefly, BMCs were after incubation with BrdU stained against corresponding combination of fluorochrome-conjugated antibodies on ice for 30 min in the dark. BMCs were then washed, fixed, permeabilized and treated with DNase (30 µg per sample) to expose incorporated BrdU. To detect the incorporated BrdU, BMCs were subsequently incubated with anti-BrdU antibody for 20 min at the room temperature in the dark. Total amount of DNA was stained by adding 20 µl 7AAD to each sample.

3.6.2 Cell cycle analysis after *in vivo* staining of DNA synthesizing cells

<u>HSPCs and myeloid progenitors (CMPs, GMPs, MEPs)</u>

To determine the cell flow rate into the G2-phase of the cell cycle, dual thymidine analogues sequential DNA-labelling was applied (Martynoga *et al.*, 2005; Massey *et al.*, 2015). The combination of EdU and BrdU was used, and the method had to be optimized for use *in vivo* (see Results part 4.2.1). EdU (1.5 mg/mouse) and BrdU (2 mg/mouse) were administered intravenously (i.v.) separated by a time interval (T_I). Bone marrow was collected into an ice-cold PBS/BSA precisely 30 minutes after BrdU administration, stained with the corresponding combinations of antibodies against surface markers. The APC BrdU Flow Kit was used to process DNA-labelled cells, similarly as suggested in the previous paragraph (3.6.1) with the exception of incorporated BrdU detection. BrdU was detected by anti-BrdU

antibody (MoBU-1 clone) that is highly specific for BrdU, and EdU detection was performed with a Click-iT^{TM} Plus EdU Alexa Fluor 488 Flow Cytometry Assay Kit chemistry. The G2 cell flow rate was indicated by the percentage of $EdU^{+}BrdU^{-}$ cells.

To determine the cell flow rate into the G1-phase of the cell cycle, mice were i.v. injected with 1 mg/mouse of BrdU, and after various time intervals (0.5-4.5 hours) bone marrow was collected into ice-cold PBS/BSA. Bone marrow cells were then stained with antibodies for the identification of various types of HSPCs, their DNA content was stained with 7AAD. The cell-bearing BrdU labels were stained with an APC BrdU Flow Kit and the percentage of diploid cells with 2n DNA content and positive for BrdU were determined by flow cytometry to distinguish between diploid G1/G0 cells and tetraploid G2 cells. The cell flow into the G1-phase was calculated from the change in the percentage of $BrdU^{+}$ diploid (2n) cells occurring in the period 1.5-4.5 hours after BrdU administration.

Erythroid progenitors and precursors

To determine the cell flow rates through the cell cycle of erythroid progenitor and precursor cells, dual thymidine analogues sequential DNA-labelling with EdU and BrdU was applied. EdU (1.5 mg/mouse) and BrdU (2 mg/mouse) were administered intravenously (i.v.) separated by a time interval of 3 hours. The APC BrdU Flow Kit was used to process DNA-labelled cells, similarly as was suggested in the paragraph 3.6.1 with the exception of incorporated BrdU detection. BrdU was detected by anti-BrdU antibody (MoBU-1 clone) that is highly specific for BrdU, and EdU detection was performed with a Click-iT^{TM} Plus EdU Alexa Fluor 488 Flow Cytometry Assay Kit chemistry. The total amount of DNA was stained by adding 20 µl 7AAD to each sample.

Colchicine (0.05 mg/mouse) was administered intraperitoneally to arrest erythroid progenitor and precursor cells in metaphase. The dual thymidine analogues sequential DNA-labelling with EdU and BrdU as described in the previous paragraph was applied 0.5 hours after the administration of colchicine.

3.7 Flow cytometry and cell sorting

Stained bone marrow cells were analysed using a digital FACS Canto II flow cytometer, and a FACSAria IIu cell sorter. BD FACSDiva software version 6.1.3 or version 8.0.1 was used for data acquisition. CS&T beads were used for the automated cytometer setup and the performance tracking procedure before measurements. The proper compensation matrix was created by running single-stained control samples (automatic compensation). The compensation matrix was then checked and manually adjusted (if necessary) at each measurement. The generated flow cytometry data were analysed using FlowJo vX software. Debris, red blood cells and dead cells were excluded from the analysis by gating the FSC-A/SSC-A dot plot. For cell doublet discrimination, a FSC-A/FSC-H dot plot was used. To properly interpret flow cytometry data, Fluorescence-Minus-One (FMOs) controls were used for gating.

For cell sorting, FACSAria IIu cell sorter was used with the sort setup: 70 µm nozzle, 70 psi sheath pressure and 0-16-0 sorting precision mode. Before sorting, the drop delay was determined by automated method with the use of Accudrop beads - RUO (BD Biosciences, USA). BD FACSDiva software version 8.0.1 was used for cell sorting.

3.8 Imaging flow cytometry

Stained bone marrow cells were analysed using 12 channels system AMNIS ImageStream X Mark II cytometer. INSPIRE system software was used for data collection. IDEAS analysis software was used for the analysis of collected data. The SpeedBead ImageStream X calibration reagent was used to calibrate the instrument before measurement by the automated suite of the systemwide ImageStreamX tests module. Fluorescence signal compensation (if necessary) was done according to the IDEAS user manual.

3.9 *In vitro* cultivation of erythroid progenitors in semi-solid media

MethoCult™ SF M3436 was used for murine erythroid BFU-E and and MethoCult™ M3334 for murine CFU-E progenitors. The BMCs were stained with fluorochrome-conjugated antibodies listed in the “Erythroid differentiation” panel (paragraph 3.1.2) and incubated on ice for 30 min in the dark. BMCs were then washed and different stages of erythroid progenitor cells were sorted and plated on 30-mm Petri dishes in 1 ml of a semi-solid medium at

concentrations of 1 x 10^3 cells/ml (SF M3436) and 2 x 10^3 cells/ml (M3334). Two dishes were used for each progenitor sample and were kept for 2 days (CFU-E) or for 12 days (BFU-E) at 37°C in a humidified atmosphere with 5% CO_2. Colonies were analysed and counted by phase contrast light microscopy and evaluated according to the STEMCELL Technologies Mouse Colony-Forming Unit (CFU) Assays Technical Manual (v 3.2.0; Document # 28405).

3.10 Statistical analysis

Statistical analysis was performed with GraphPad Prism version 5 (GraphPad Software, CA, USA). Values in graphs are presented as mean ± standard error of the mean (SEM), values in tables are presented as mean ± standard deviation (SD). Two-way analysis of variance (ANOVA) was used to compare each group to the control group. One-sample, two-tailed Student´s t-test was used to evaluate statistical significance against the theoretical expected values. P values <0.05 were considered statistically significant. * P<0.05; ** P<0.01; *** P<0.001.

4 Results

4.1 Determination of DNA synthesizing cell fraction in HSPC subpopulations

4.1.1 Flow cytometry analysis of HSPC subpopulations

Flow cytometry method was used to study early developmental stages of haematopoietic cells. The bone marrow cells were divided according to the expression of the Sca-1 marker into Sca-1$^+$ (LSK) and Sca-1$^-$ (LS$^-$K) subpopulations. LSK cells were further divided into four subpopulations according to their CD150 and CD48 expression patterns: haematopoietic stem cells (HSCs) CD150$^+$CD48$^-$, multipotent progenitors (MPPs) CD150$^-$CD48$^-$, and heterogeneous restricted progenitors (HPCs-1 and HPCs-2) CD150$^-$CD48$^+$ and CD150$^+$CD48$^+$, respectively (Kiel *et al.*, 2005; Oguro, Ding and Morrison, 2013). LS$^-$K cells lacking IL7R were characterized by CD34 and CD16_32 (FcγR III/II) markers as CMPs (common myeloid progenitors), GMPs (granulocyte-macrophage progenitors) and MEPs (megakaryocyte-erythroid progenitors) (Akashi *et al.*, 2000) (for gating see Figure 5).

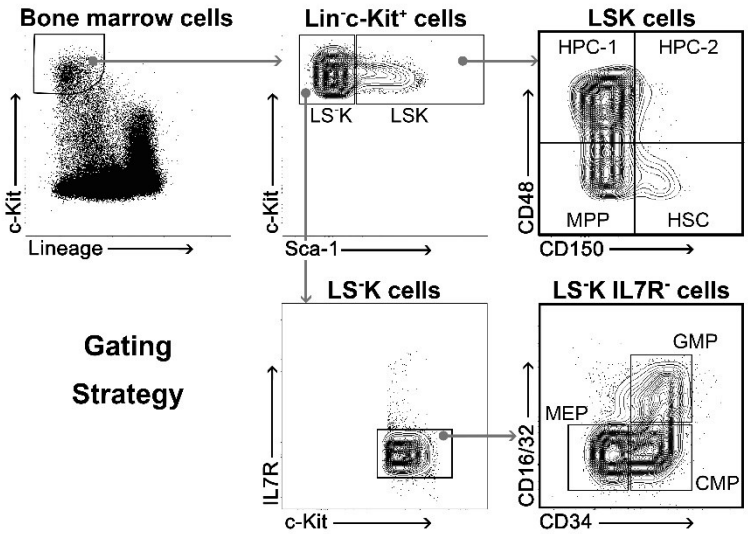

Figure 5 - Representative flow-cytometry analysis of HSPCs in murine bone marrow cells

Lin$^-$c-Kit$^+$ cells: Lineage negative c-Kit positive immature cells

LSK cells: Lin$^-$c-Kit$^+$ cells expressing Sca-1 antigen

LS$^-$K cells: Lin$^-$c-Kit$^+$ cells lacking Sca-1 antigen

LS$^-$K IL7R$^-$ cells: LS$^-$K cells lacking receptor for IL7 (interleukin 7)

4.1.2 The fraction of DNA-synthesizing cells is a characteristic feature of HSPC subpopulations

We determined pulse BrdU incorporation into immature bone marrow cells lacking lineage markers (Lin^-) and highly positive for c-Kit ($Lin^-c\text{-}Kit^+$ cells) in 8 independent experiments, using 8 male and 8 female C57BL/6J mice in total.

The BrdU positive cells indicating the S-phase fraction of DNA-synthesizing cells ranged from 2.5±0.6% in MPPs to 64.8±2.3% in MEPs (Figure 6A, B). There was no significant difference in the percentage of cells in the S-phase between male and female mice.

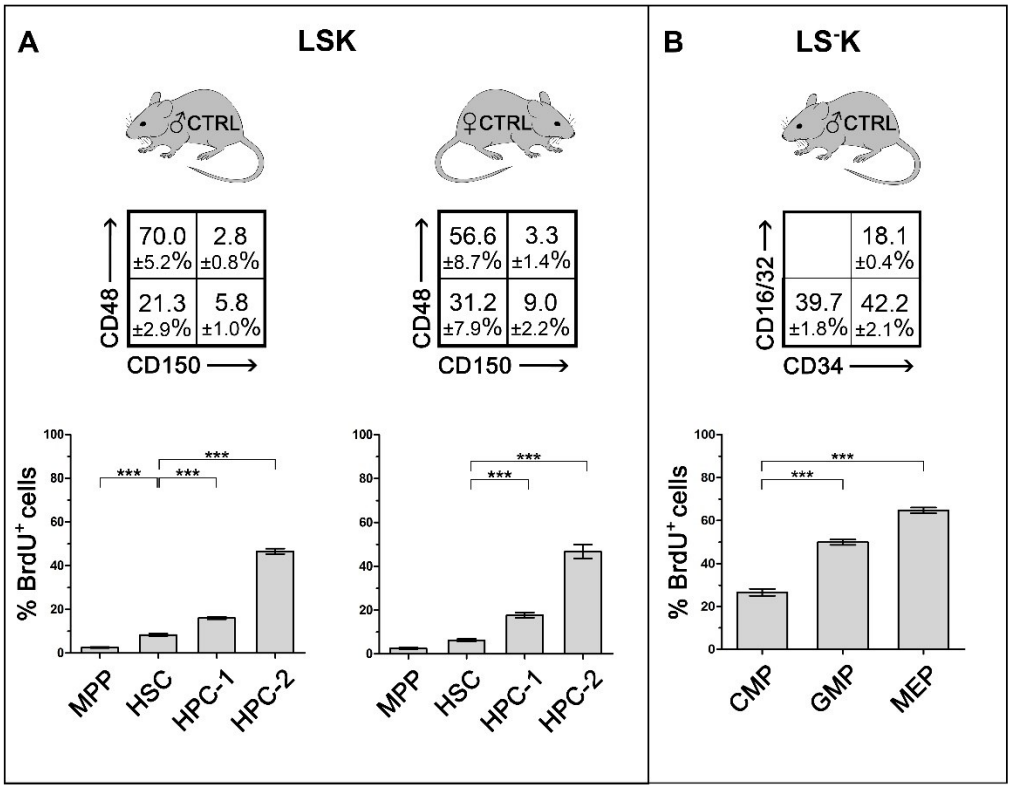

Figure 6 - Frequency and proliferation rate of various subtypes of LSK and LS^-K cells

A) *The frequency of HSC, MPP, HPC-1, HPC-2 in bone marrow of 8 male and 8 female mice and their $BrdU^+$ (S-phase) fraction after forty-five-minutes in vitro exposure to BrdU. Significant differences to HSCs ($CD150^+CD48^-$ cells) are marked *** ($p<0.001$)*

B) *The proportion of CMP, GMP and MEP cells in bone marrow of 4 male mice and their $BrdU^+$ (S-phase) fraction after forty-five-minute in vitro exposure to BrdU. Significant differences to CMPs are marked *** ($p<0.001$).*

4.1.3 The HSPC proliferation hierarchy is age and sex independent

To check the consistency of these proliferation characteristics of various types of immature haematopoietic cells, we analysed LSK subpopulations in an additional four independent experiments comprised of untreated male and female mice of various ages (Figure 7). Interesting is the very low proliferation rate in relatively abundant MPPs which has been a constant finding through our experiments.

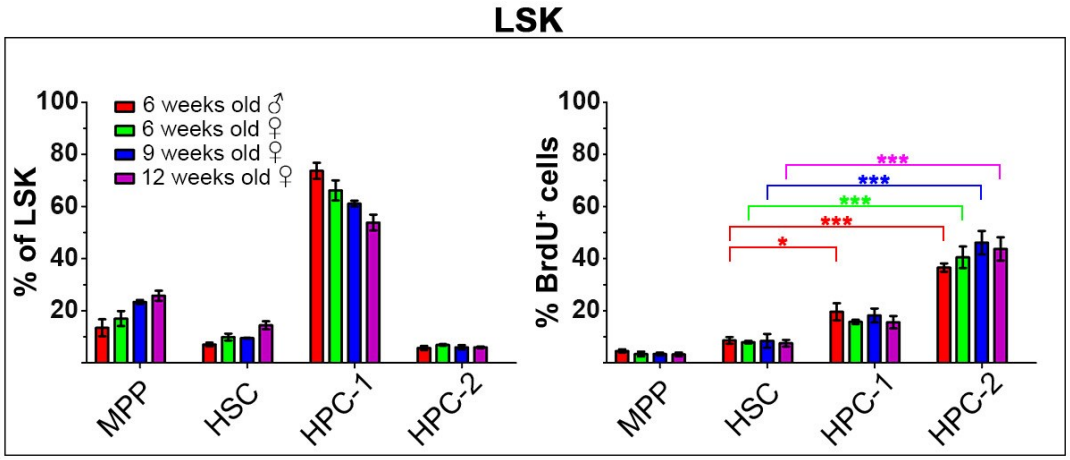

Figure 7 - Frequency of four CD150/CD48 subpopulations of LSK cells and their proliferation rate assessed according to percentage of BrdU-positive cells.

*Difference in % of BrdU-labelled cells was evaluated in all subpopulations compared HSCs. Significant differences from HSCs are marked *p<0.001,***p<0.001.*

4.2 Cell cycle kinetics in HSPC subpopulations

4.2.1 Refinement of the EdU-BrdU technique for determination of the HSPC cell flow rate into the G2-phase of the cell cycle

We used the dual EdU-BrdU labelling technique to determine the duration of S-phase (T_S), cell flow rate into the G2-phase, and an average duration of the cell cycle (T_C) to further characterize the cell cycle features of HSPCs and to estimate their production rate. To avoid a prolonged incubation of bone marrow in the presence of halogenated DNA-labelling compounds and obtain thus data for cells imbedded in their natural tissue microenvironment, we decided to label HSPCs by injecting EdU and BrdU to mice *in vivo*. The sequential labelling procedure with EdU and BrdU had to be optimized, due to the fact that the duration of the drugs' availability after their administration was unknown.

EdU and BrdU injection were separated by a time interval T_I and bone marrow cells were collected 0.5 hours after BrdU injection. The EdU^+BrdU^- cell fraction represents the cells leaving the S-phase during T_I, while the EdU^-BrdU^+ cell fraction represents the cells entering the S-phase after BrdU administration. With T_I set at 2 hours (Figure 8A), the ratio between EdU^+BrdU^- and EdU^-BrdU^+ (E/B ratio) cells ranged from 0.97 to 1.64 (Figure 8D, left column). This was significantly less than its expected value of 4.0 corresponding to the fourfold longer time after EdU administration compared to that after BrdU administration. This demonstrated that EdU was not available to DNA synthesizing cells for the entire 2-hour period preceding BrdU administration.

To achieve the labelling of all DNA synthesizing cells with EdU, i.e. those synthesizing DNA at the time of EdU administration and those which initiated DNA synthesis during the T_I interval preceding BrdU administration, we injected mice with a second dose of EdU 0.5 hours before injecting BrdU (see Figure 8B). With this modification the E/B ratio slightly exceeded the theoretical value of 4.0 when T_I was still set at 2 hours. We hypothesized that this E/B ratio exceeding 4.0 was caused by overestimation of the EdU^+BrdU^- cell fraction due to mitotic division in some of these cells during 2.5 hours after the first EdU dose. After shortening T_I to 1.5 hours, the E/B ratio achieved the expected theoretical value of 3.0 (Figure 8D middle and right columns). Figure 8C shows representative EdU-BrdU plots for the three experimental settings.

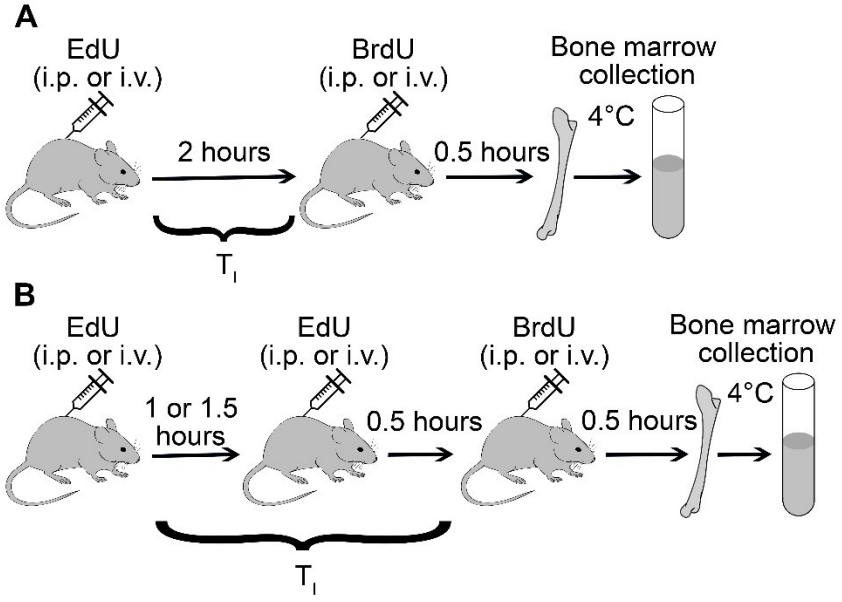

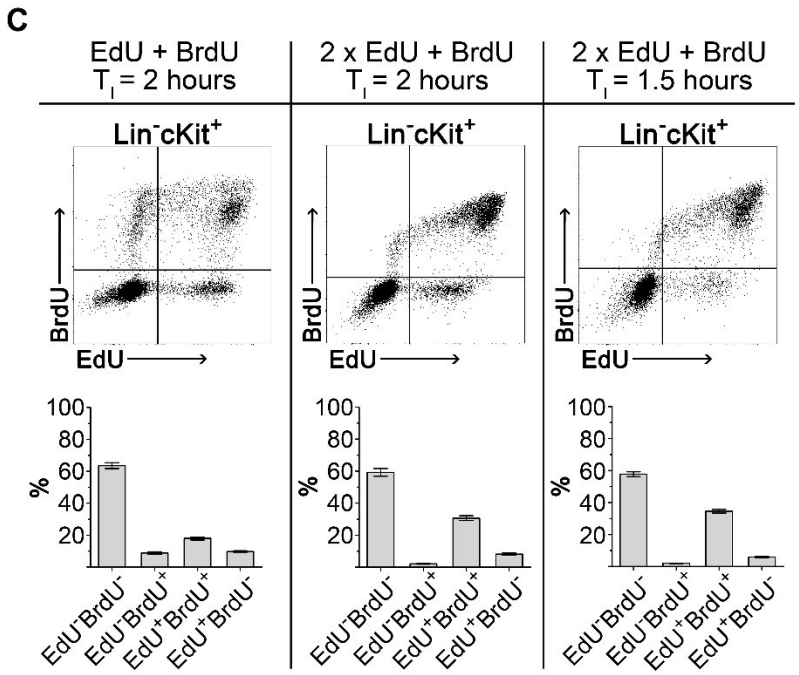

D

	(EdU⁺BrdU⁻) / (EdU⁻BrdU⁺) ratio		
	T_I = 2 hours expected value = 4		T_I = 1.5 hours expected value = 3
	EdU + BrdU	2 x EdU + BrdU	2 x EdU + BrdU
LSK	1.47 ± 0.85	4.47 ± 0.18	2.98 ± 0.19
LS⁻K	1.11 ± 0.15	4.64 ± 0.12	2.97 ± 0.04
CMP	1.64 ± 0.34	4.72 ± 0.11	3.00 ± 0.07
GMP	1.97 ± 0.39	4.63 ± 0.15	2.96 ± 0.15
MEP	0.97 ± 0.03	4.57 ± 0.10	2.97 ± 0.09

Figure 8 - Optimization of EdU-BrdU dual labelling technique applied to HSPC *in vivo*

A) *Dual-deoxynucleoside labelling with single EdU (1.5 mg/mouse) and single BrdU dose (2 mg/mouse) separated by 2 hours (T_I). Bone marrow cells were harvested 0.5 hours after BrdU administration.*

B) *Dual-deoxynucleoside labelling with two doses of EdU (2 x 1.5 mg/mouse) and single dose of BrdU (2 mg/mouse).*

C) *Representative dot-plots of Lin^-cKit^+ cells and EdU/BrdU fractions frequency in three experimental settings.*

D) *Ratio of S-phase exiting cells (EdU^+BrdU^-) to S-phase entering cells (EdU^-BrdU^+) in three experimental settings determined in LSK cells, LS^-K cells and their CMP, GMP and MEP subpopulations. Four to six mice were analysed in each of the experimental settings. The experimentally obtained ratios were tested by Student's t-test (one sample, two-tailed) to the expected theoretical ratio of 4.0 or 3.0 (see text). The ratios were significantly different ($P<0.05$) from 4.0 in the left two columns. Results in the table are mean ± SD.*

The optimized DNA labelling method, using two doses of EdU given 1 hour apart and T_I set at 1.5 hours, is graphically shown in Figure 9. This experimental setting has been further used to determine the duration of the S-phase in various types of HSPCs, the cell flow rate into the G2-phase of the cell cycle, and for calculating the duration of their cell cycles.

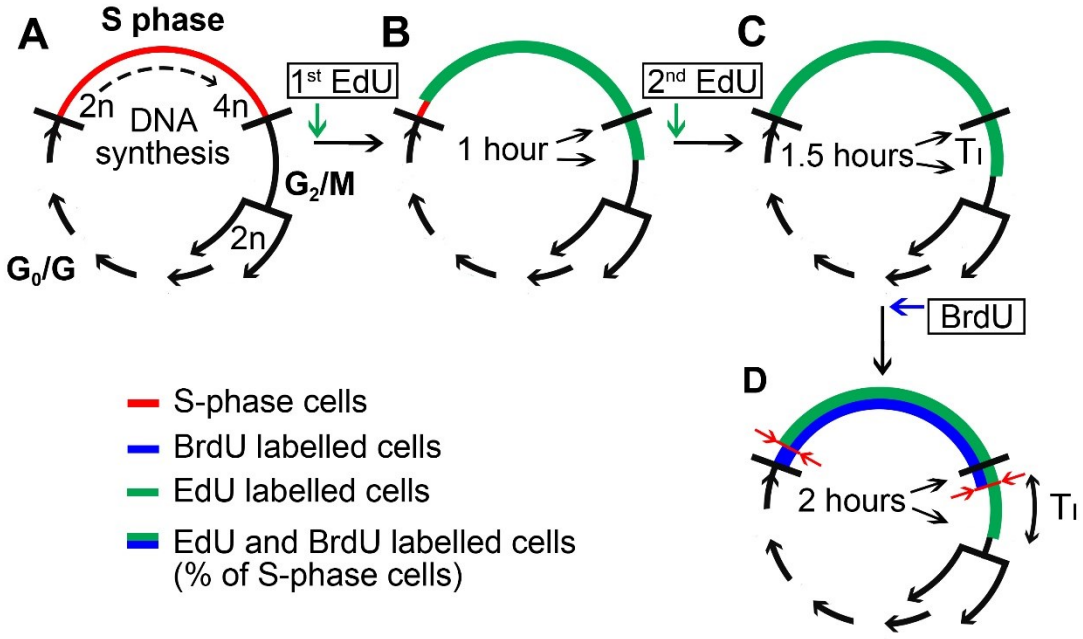

Figure 9 - EdU – BrdU dual labelling of DNA optimized for *in vivo* cell cycle analysis of HSPCs (2 x EdU, T_I = 1.5 hours).

A) *Cell cycle with highlighted S-phase (red)*

B) *EdU labels DNA (green) 0.5 hours after its administration and there are EdU unlabelled cells at the beginning of S-phase one hour after EdU (red)*

C) *2nd EdU dose, given 0.5 hour before BrdU, ensures that all DNA-synthesizing cells are labelled with EdU (green) during T_I*

D) *Half an hour after BrdU, all S-phase cells are double labelled by both EdU (green) and BrdU (blue). EdU-only labelled cells indicate the cells that exited from the S-phase during T_I.*

4.2.2 Cell flow rate into the G2-phase and S-phase duration in HSPCs

The labelling of cells with EdU and BrdU in the cell nucleus in parallel with the staining of cell membrane markers was verified by imaging flow cytometry (Figure 10A).

The G_2 flow rate and the S-phase cell duration were determined according the equation in the Figure 10B in all LSK cells and all LS^-K cells, in the LS^-K cells also in their three subtypes: CMPs, GMPs and MEPs. The S-phase duration ranged from 6.3±0.5 hours in GMPs to 9.8±0.7 hours in MEPs (Figure 10C).

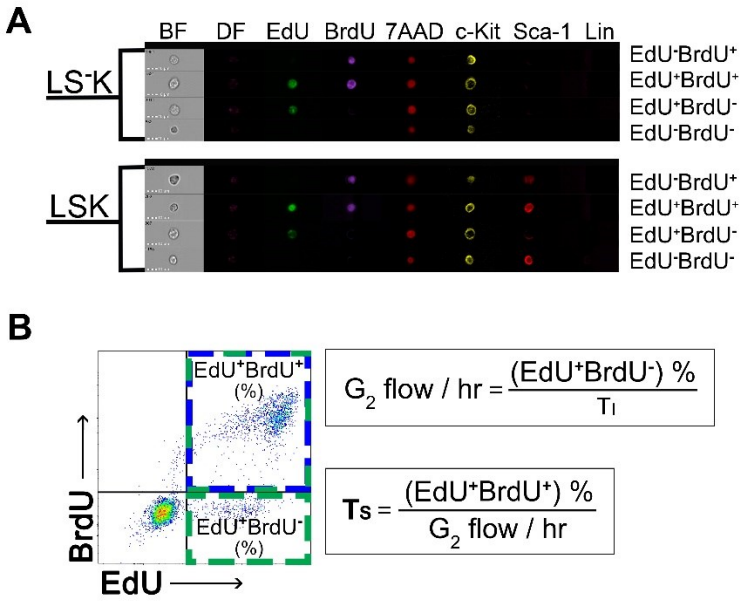

C

	LSK	LS-K	CMP	GMP	MEP
G_2 flow / hour	2.2 ± 0.2	4.3 ± 0.5	2.4 ± 0.4	4.0 ± 0.4	6.0 ± 0.5
S-phase (hours)	7.8 ± 0.7	8.7 ± 0.6	8.7 ± 1.2	6.3 ± 0.5	9.8 ± 0.7

Figure 10 - EdU-BrdU dual labelling of LSK and LS$^-$K cells and its use to estimate duration of the S-phase

A) *Representative example of surface antigen staining of Lin$^-$c-Kit$^+$ cells combined with DNA labelling with EdU and BrdU as shown by imaging flow cytometry. 7AAD was used as a nuclear marker.*

B) *Representative example of Lin$^-$c-Kit$^+$ cells plotted on EdU vs. BrdU diagram with color-highlighted gates (EdU$^+$BrdU$^-$ in the green gate, EdU$^+$BrdU$^+$ in the green/blue gate) corresponding to the EdU-BrdU labelling scheme depicted in Figure 9. The EdU$^+$BrdU$^-$ cells indicate the fraction of S-phase cells exiting the S-phase and thus entering into the G_2-phase within 1.5 hours (T_I) i.e. the G_2 cell flow rate. The total number of S-phase cells is indicated by EdU$^+$BrdU$^+$ cells (see part 4.2.1 of Results). The S-phase duration (T_S) is then calculated according the above equation.*

C) *G_2 cell flow rate and duration of S-phase (T_S) were determined in six mice (female) given two doses of EdU and a single dose of BrdU with a T_I = 1.5 hours (see Figure 8B). The results in the table are mean ± SD from the six mice analysed also in Figure 8.*

4.2.3 Cell cycle duration in HSPCs

Assuming that all cells proliferate, the G2 flow rate (see table in Figure 10C) was used also for the calculation of the average cell cycle duration (Tc) in various types of HSPCs (Figure 11).

A

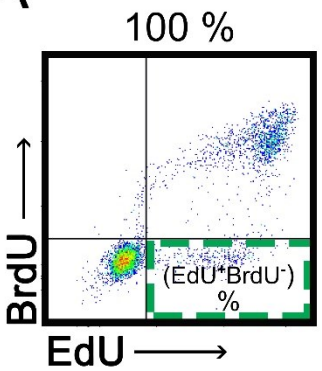

$$Tc = \frac{100\ \%}{G_2\ \text{flow / hr}} \ *$$

* all cells are proliferating

B

	Average Tc (hours)
LSK	47.0 ± 4.9
LS-K	23.4 ± 2.3
CMP	42.5 ± 7.3
GMP	24.9 ± 2.2
MEP	16.7 ± 1.3

Figure 11 - Average cell cycle time in LSK and LS-K cells

A) *The cell cycle time (T_C) is calculated as 100% (all cells of the explored population) / G_2 cell flow rate per hour (%). The T_C values thus represent an average values of cell cycle duration under the simplification assuming that all cells continuously cycle.*

B) *Duration of cell cycle (T_C) was determined in six mice (female) given two doses of EdU and a single dose of BrdU with T_I = 1.5 hours (see Figure 8B). Results are mean ± SD from six mice analysed also in Figures 8 and 10.*

4.2.4 Cell flow rate of DNA labelled cells arising from mitosis

Further, we estimated the number of *Lin*$^{-}$*c-Kit*$^{+}$ cells generated by the mitotic division of cells previously labelled in the S-phase of the same cell cycle. Figure 12C shows how the flow rate of this cells can be determined. We labelled DNA-synthesizing cells in mice with a single dose of BrdU injected 0.5 - 4.5 hours prior to bone marrow collection and examined BrdU^{+} cells with the diploid (2n) DNA content. DNA-synthesizing cells incorporate BrdU only for a short time after BrdU *in vivo* administration (approx. 0.5 hours). After this time, the cells entering into the S-phase do not incorporate BrdU and the percentage of BrdU labelled cells decrease in the initial part of the S-phase when cells still have ≈ 2n DNA content. Only when the cells which have incorporated BrdU during the final part of the S-phase pass the G2-phase and mitotically divide, a new wave of 2n BrdU^{+} cells appears and progressively increases as the cells which have incorporated BrdU in the middle and the early parts of S-phase divide and give rise to BrdU^{+} cells with a 2n DNA content.

BrdU^{+} diploid cells appeared 1.5 hours after BrdU administration (Figure 12A, B) and their number increased linearly until 4.5 hours (Figure 12D). The slope of the linear regression reflecting the increase in the 2n BrdU^{+} cell number, after its nadir corresponding to the duration of G2-phase and mitosis, reflects cells produced by mitotic division from those which have had incorporated BrdU at the time of its administration and, importantly, preserved the same phenotype after division (Figure 12D).

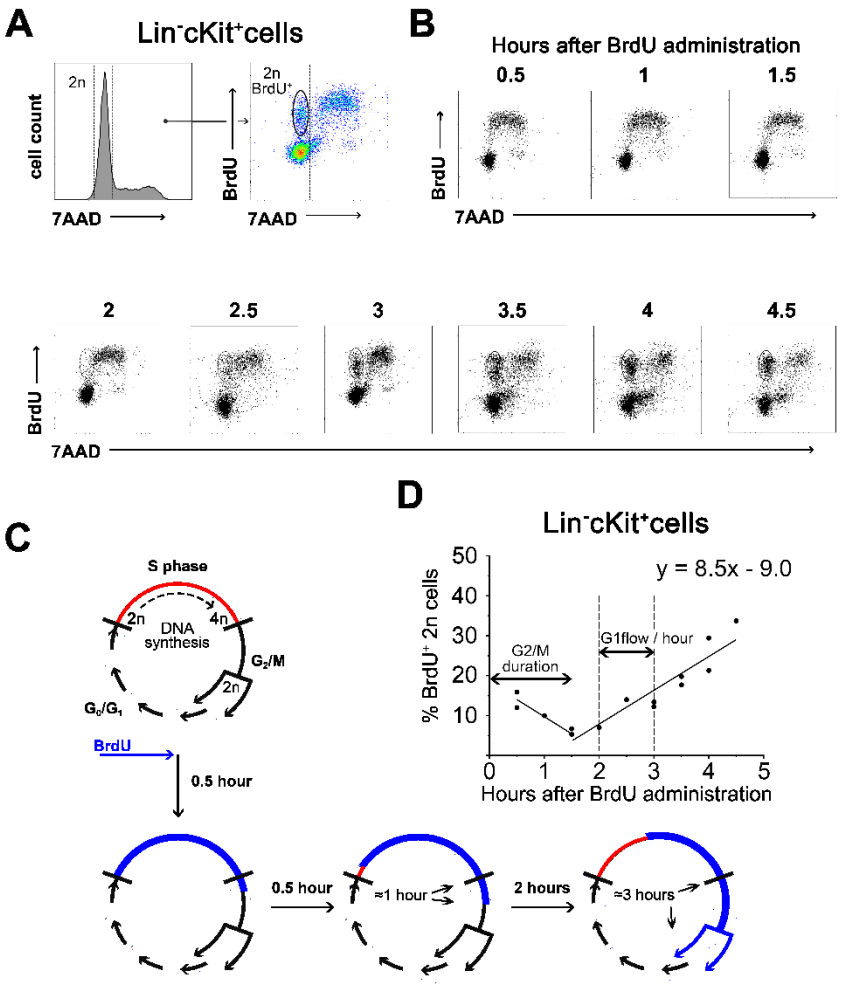

Figure 12 - BrdU labelled diploid (2n) Lin$^-$cKit$^+$ in bone marrow collected between 1.5-4.5 hours after a single dose of BrdU

A) *Representative 7AAD histogram and BrdU / 7AAD dotplot of Lin$^-$cKit$^+$ cells depicting gating strategy for 2n daughter cells.*

B) *Representative examples of diploid (2n) BrdU$^+$ daughter cell appearance in the population of Lin$^-$c-Kit$^+$ bone marrow cells collected and analysed in increasing time intervals after BrdU administration (i.v., 1.5 mg/mouse).*

C) *Schematic image showing the principle of measuring of the cell outflow from mitosis (red: cells with unlabelled DNA, blue: cells with BrdU-labelled DNA).*

D) *Results of the analysis of Lin$^-$c-Kit$^+$ bone marrow cells. Changes in 2n BrdU$^+$ cells frequency depending on time elapsed since BrdU administration. Results from three independent experiments were pooled. The points were fitted to a line by linear regression, and the equation of increasing line is listed in graph (n=15).*

4.2.5 Cell numbers generated by mitotic division do not correspond to the number of cells entering G2-phase

We determined the flow rates of 2n BrdU$^+$ cells for all HSPC subpopulations according to the curve slopes of the linear regressions reflecting the increase in the 2n BrdU$^+$ cell number as described in the previous chapter (4.2.4.) (Figure 13A).

Our expectation that the increment in 2n BrdU$^+$ cells per hour, i.e. the cell flow rate into the (G0)G1-phase, should be twice as high as the cell flow rate into the G2-phase in particular cell types, due to the doubling effect of mitosis was not confirmed. Our experimental data differed from this theoretical value of 2.0 both in LSK cells, where it was only 1.1, and also in LS$^-$K cells, where it was 2.4-2.9 (Figure 13B).

A

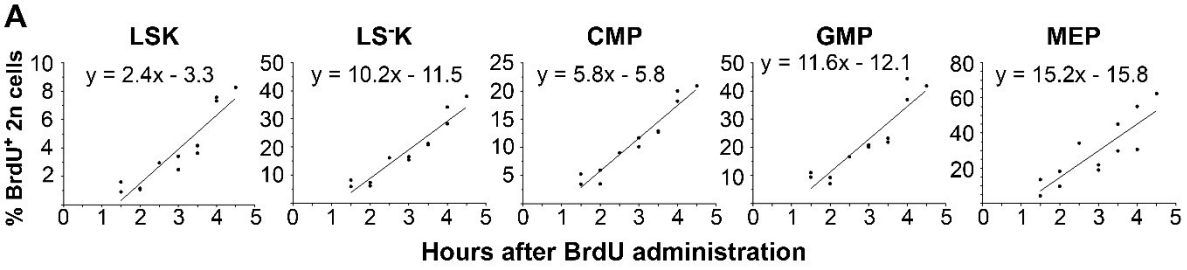

B

	LSK	LS$^-$K	CMP	GMP	MEP
2n BrdU$^+$ per hour (%)	2.4	10.2	5.8	11.6	15.2
2n BrdU$^+$ / EdU$^+$BrdU$^-$ ratio	1.1	2.4	2.4	2.9	2.6

Figure 13 - Flow rate of 2n BrdU$^+$ cells entering into the (G0)G1-phase determined in HSPCs

A) *Changes in 2n BrdU$^+$ cells frequency depending on time elapsed since BrdU administration. Results from three independent experiments were pooled. The points were fitted to a line by linear regression, and the equations of increasing line are listed in graphs (n=12)*

B) *2n BrdU$^+$ increment per hour, i.e. G1 flow rate, determined according to curve slopes and ratio of G1 flow rate vs G2 flow rate for each HSPC type.*

4.2.6 Estimation of cell production in HSPCs

Previous results showed that almost half of LSK cells lost the Sca-1 antigen after mitotic division because the cell flow rate into G1-phase was only 1.1 times that in the preceding G2 phase, instead of the expected value of 2.0. This corresponds to asymmetric cell division where one cell replaces the cell that had divided and the other cell differentiates into another (LS^-K) cell type. In contrast, in LS^-K cells and in their CMPs, GMPs and MEPs subtypes, the cell flow rate into the G1-phase was more than 2.0 times that in the preceding G2 phase, which indicated that a majority of the LS^-K cells arising from mitotic division entered a new round of the cell cycle while both preserving their phenotype, i.e. the mitosis was symmetric and self-renewing. Furthermore, there is indication for an additional external influx of LS^-K cells, presumably from a part of LSK cells that lost Sca-1 marker after/during mitosis. This interpretation of our experimental data analysing the flow rate of LSK and LS^-K cells into the G2- and G1/G0 phases, essential for estimation of the cell production rates in LSK and subtypes of LS^-K cells, is shown diagrammatically in Figure 14A.

The calculation of cell production rates used the total number of a particular cell type in bone marrow (N) determined from the number of the cells in the femoral bone marrow multiplied by 15 (bone marrow in 1 femur represents ≈ 6.7% of the total bone marrow (Novak and Necas, 1994))

Other experimentally determined values used for estimation of the cell production rate in subtypes of $Lin^-c\text{-}Kit^+$ immature haematopoietic cells were their cell flow rates into the G2-(G2) and G1-phases (G1) of the cell cycle and the G1/G2 ratio (R). The cells produced per hour in the entire bone marrow are then calculated as N x G2 x R/100. The estimates of the cells produced in LSK cells and three types of LS^-K cells are presented in Figure 14B. For comparison, the estimate of the total production of the mature myeloid cells derived from their numbers in blood and their replacement rates (Novak and Necas, 1994; Necas *et al.*, 1995) is presented as well.

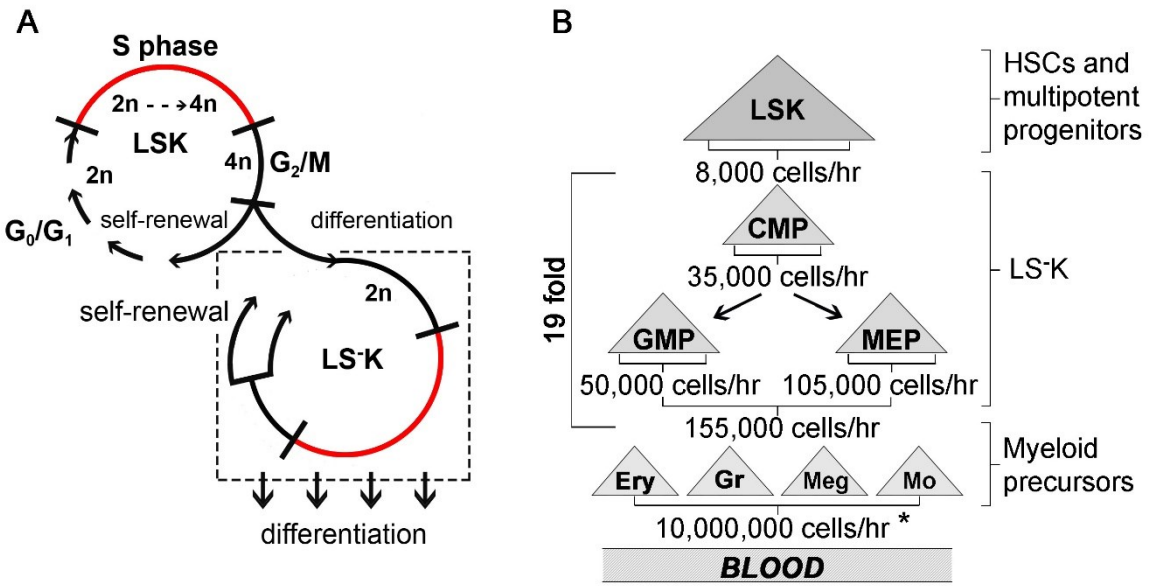

Figure 14 - A model of self-renewal and differentiation in LSK and LS$^-$K cells and estimation of cell production in hierarchy of HSPCs and myeloid precursors of blood cells

A) *Cell division in LSK cells is primarily asymmetric when one cell becomes an LS$^-$K cell, while the other enters a new self-renewing cell cycle. LS$^-$K cells undergo self-renewal leading to their amplification and receive an influx of cells from the asymmetrically dividing LSK cells. The differentiation of LS$^-$K cells is not linked to cell division.*

B) *Developmental hierarchy within HSPCs with established cell production rates and the average multiplication factor in the compartment of LS$^-$K cells and in the maturing precursors of red blood cells, granulocyte/monocytes and megakaryocytes. The cells produced per hour are calculated as described in Results. Briefly, the absolute number of various types of HSPCs determined in the femoral bone marrow was multiplied by 15 to estimate their absolute numbers in whole bone marrow (N). This was multiplied by the cell flow rate into G2-phase (G2) (see Figure 10) and further by the ratio of the cell flows in G1- and G2-phases of the cell cycle (see Figure 13) reflecting their mitotic multiplication efficiency. *estimated in Novak & Necas 1994 and Necas et al., 1995.*

4.3 Cell cycle and differentiation of erythroid progenitor and precursor cells

4.3.1 Imaging flow cytometry analysis of erythroid progenitor and precursor cells

We have established a new approach for identifying individual erythroid-progenitor stages within bone marrow cells.

We discriminated erythroid progenitors in bone marrow cells lacking the expression of the lineage markers (B220, Gr-1, Mac-1), the marker of immature HSPCs (Sca-1) and the granulocyte-macrophage-progenitor marker (CD16_32). These $B220^-/Gr\text{-}1^-/Mac\text{-}1^-/Sca\text{-}1^-/CD16\_32^-$ bone marrow cells were then divided into 10 erythroid-progenitor gates according to their c-Kit and CD71 expression (Figure 15A).

The cells in gates 0 – 5 were investigated for their capacity to form erythroid colonies. Cells in gate 0, immunophenotypically corresponding to CMPs and MEPs, exhibited the highest BFU-E potential that was decreased in gate 1 and lost in gate 2. The highest CFU-E potential was possessed by cells in gate 1 and also lost in gate 2 (Figure 15B).

To further characterise the progenitors and nucleated precursors of red blood cells, we used the imaging flow cytometry technology and cell criteria established by McGrath et al. (2008). This approach is an alternative to the traditional microscopic classification of erythroid progenitors and enables erythroid progenitors to be distinguished according to the changes in their cell size, density of the surface-expressed antigen Ter119, in their nuclear size, and in the intensity of Draq5 stained DNA, reflecting the degree of nuclear condensation (Figure 15C, E). Figure 15D, E projects erythroid progenitor and precursor cells in gates 0 - 9 into the fields established by McGrath et al. (2008) for various developmental stages of nucleated precursors of red blood cells. Cells from gates 0 – 2, highly expressing c-Kit together with the initiation of CD71 expression, increase their cell and nuclear size and gradually differentiate into proerythroblasts (ProE). Cells from gates 3 – 4 lose c-Kit and initiate a strong Ter119 expression. They progress to the stage of basophilic erythroblasts. Cells in gates 5 – 9 progressively reduce their CD71 expression, shrink the cell and nuclear sizes, pass through the stage of polychromatic erythroblasts to the last nuclear erythroid precursor: orthochromatic erythroblasts. Moreover, the presence of pyrenocytes in the gates 7 – 9 suggests the onset of enucleation.

It should be noted that the identification of erythroid progenitors and differentiated precursors by imaging flow cytometry remains to a certain extent subjective because erythroid differentiation is a mostly continuous process that does not occur in easily identifiable discrete differentiation steps.

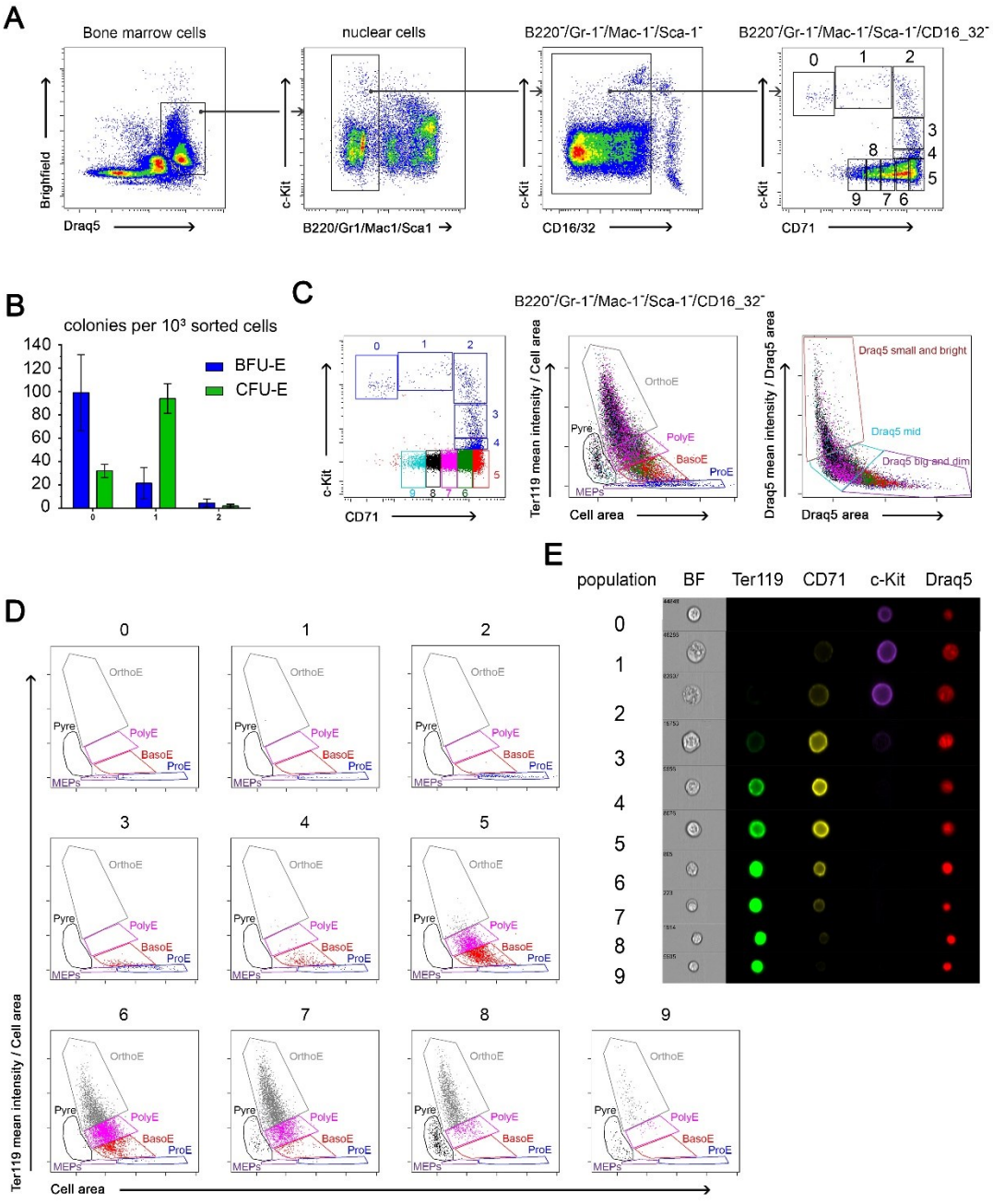

Figure 15 - Identification of erythroid progenitor and precursor cells in bone marrow

A) *Representative flow-cytometry analysis of erythroid progenitor and precursor cells in murine bone marrow.*

B) *BFU-E and CFU-E colony-forming potential of cell in gates 0 – 5. 10^3 sorted cells from each of gates 0 - 5 were in vitro cultured in duplicates on a 30-mm Petri dish in a culture medium optimized for burst-forming unit-erythroid (BFU-E, SF M3436 medium). $2x10^3$ sorted cells from each of gates 0 - 5 were in vitro cultured in duplicates on a 30-mm Petri dish in a culture medium optimized for colony-forming unit-erythroid (CFU-E, M3334 medium). BFU-E colonies*

were scored on day 12, CFU-E colonies on day 2. Results are pooled from two independent experiments.

C) *The B220$^-$/Gr-1$^-$/Mac-1$^-$/Sca-1$^-$/CD16_32$^-$ bone marrow cells were analysed according to their changing cell size (middle dot-plot) and progressive nuclear condensation (right dot-plot). This gating strategy for distinguishing nuclear erythroid progenitor and precursor cells was adopted from the study published by* McGrath et al. (2008).

D) *The appearance of developmental stages of nuclear erythroid progenitor and precursor cells in individual gates 0 – 9.*

E) *Representative examples of erythroid progenitor and precursor cells identified in gates 0 - 9.*

4.3.2 Progression of erythroid progenitor and precursor cells through S-phase of the cell cycle and its association with cell differentiation

To examine the cell cycle status of erythroid progenitors and precursors, we administered i.v. BrdU to mice and harvested bone marrow after 30 min. The bone marrow was processed to show the BrdU cell labelling against their DNA content, which doubled during the S-phase of the cell cycle from 2n to 4n. Bone marrow was also stained with fluorescently labelled antibodies which enabled us to focus the analysis on various stages of erythroid differentiation (for gating strategy see Figure 15A).

Figure 16A shows the cell cycle status in erythroid progenitors and precursors divided according to their c-Kit and CD71 expression into ten gates. For a more detailed analysis of the cell cycle within each gate, we divided the S-phase cell fraction into 3 parts according to the increasing amount of synthesized DNA: early S-phase cells, middle S-phase cells and late S-phase cells. The S-phase cells were relatively uniformly distributed in its early, middle and late parts except for the cells in gates 2 – 4. While the cells from gates 2 and 3 were in the early and middle S-phase, cells from gate 4 were mostly in the late S-phase (and G2/M-phase) (Figure 16A, B). These findings strongly suggest that the transition of cells from gate 2 to gate 4 occurs during their passage through the S-phase of a single cell cycle.

Further, we determined the mean fluorescence intensity (MFI) of fluorochrome-conjugated antibodies against CD71, c-Kit and Ter119 antigens in the cells from gates 0 – 9. Figure 16C, D shows the close correlation between the expression level of CD71 and the percentage of cells in the S-phase. The S-phase fraction increased from 7.8 ± 1.8 % in cells from gate 0 to > 90 % in cells with the highest CD71 expression level (gates 2 – 5). The S-phase fraction then declined together with diminishing CD71 expression in cells from gates 6 – 9. The expression of c-Kit is, after its initial up-regulation in cells in gates 1 and 2, strongly down-regulated in gate 3 when cells synthesize DNA in the early and middle part of the S-phase. There is a rapid onset of Ter119 expression in cells which progressed into the late S-phase in gate 4 (Figure 16C, D).

These results suggest that increased CD71 expression and initiation of DNA synthesis in the early S-phase are required for the differentiation of cells from the MEP stage to proerythroblasts appearing in gate 2 (Figure 15D) and that the differentiation of proerythroblasts into the basophilic erythroblasts present in gate 4 is associated with a steep

loss of c-Kit expression during the progression of cells through the S-phase. In contrast, Ter119 was rapidly up-regulated during this S-phase.

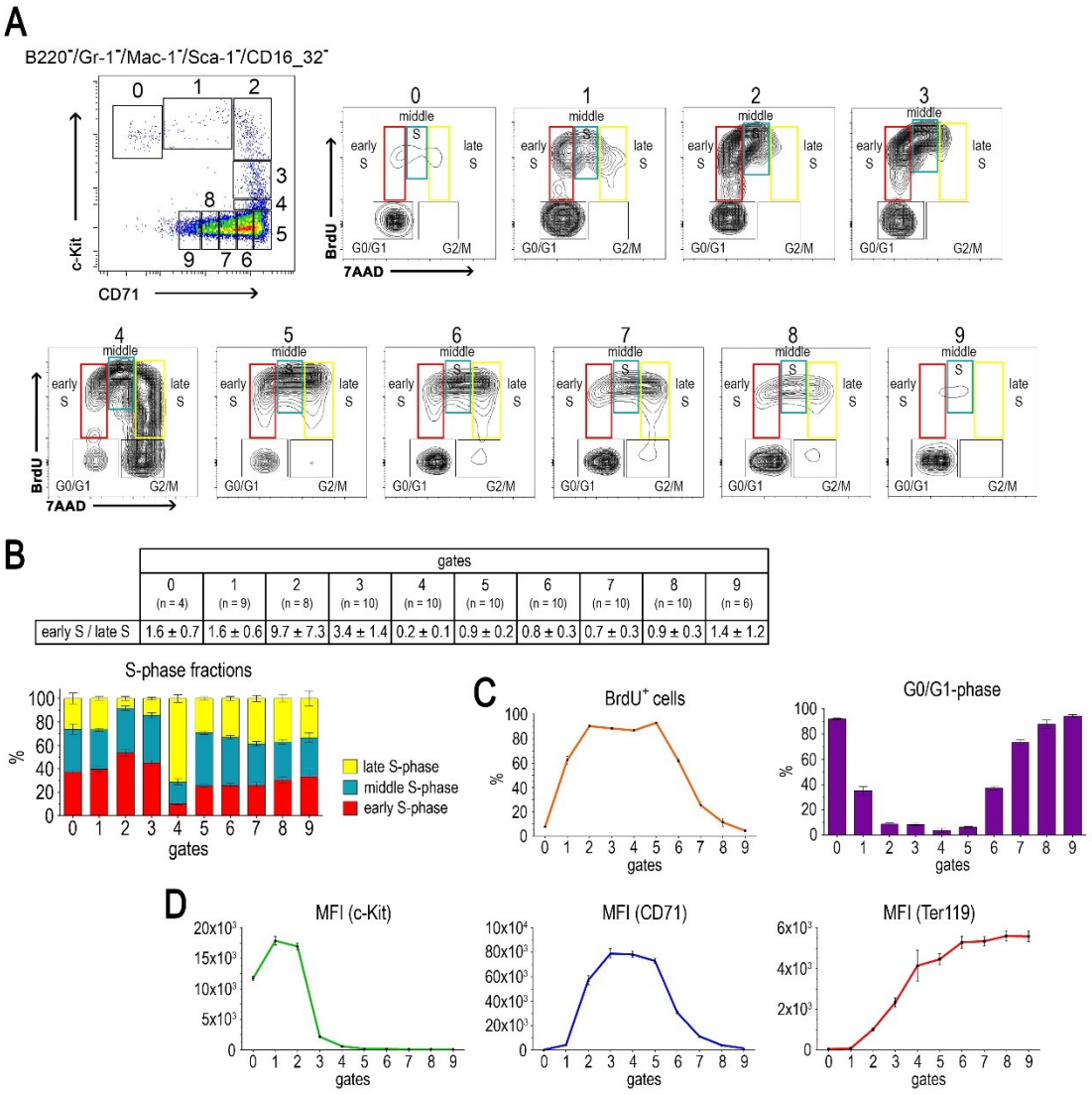

Figure 16 - Cell cycle analysis of erythroid progenitor and precursor cells

A) *B220⁻/Gr-1⁻/Mac-1⁻/Sca-1⁻/CD16_32⁻ bone marrow cells were divided according to their c-Kit and CD71 expression into ten gates (0 – 9) containing erythroid progenitor and precursor cells and their cell cycle status is depicted in representative 7AAD / BrdU dotplots.*

B) *Relative distribution of early, middle and late stages of S-phase determined in erythroid progenitor and precursor cells from gates (0 – 9), the corresponding ratios of the early S-phase cell fraction to the late S-phase are shown in the table. The results in the table are mean ± SD.*

C) *BrdU⁺ (S-phase) cell fraction frequency and G0/G1cell fraction frequency determined in erythroid progenitor and precursor cells in gates (0 – 9) (n=10).*

D) *Mean fluorescence intensity (MFI) of c-Kit, CD71 and Ter119 was analysed in erythroid progenitor and precursor cells in gates (0 – 9) (n=4).*

4.3.3 Dynamic cell cycle analysis in cells initiating the erythroid developmental pathway

From the results presented in section 4.2 of Results and published in Páral et al. (2018), we concluded that Sca-1$^-$ myeloid progenitor cells divide by symmetric self-renewing cell division and differentiate in the course of the cell cycle. To clarify how CD71$^-$ megakaryocyte-erythroid progenitor (MEP) cells develop into Ter119$^+$ erythroid cells and how this is linked to the progression of the cells through the cell cycle, we double-labelled DNA-synthesizing cells with EdU followed by BrdU 3 hours later and analysed the distribution of the labelled cells in progressively differentiating erythroid cells from their CD71$^-$ early progenitor stage (megakaryocyte-macrophage progenitor; MEPs) through CD71$^+$c-Kit$^+$ erythroid progenitors into CD71$^+$c-Kit$^-$ erythroid cells, in gates 1 - 4 (Figure 15A).

The time interval of 3 hours that separated the EdU and BrdU administration was chosen to allow the passage of the cells labelled with EdU at the end of the S-phase through the G2- and M-phases and into postmitotic cells with their DNA content reduced from 4n to 2n and thus clearly distinguishable (EdU labelled diploid cells) (Figure 17A).

The BrdU vs. 7AAD diagram is a snapshot of cells taken 0.5 hours after BrdU injection, which shows their actual distribution into the G0/G1- S- and G2/M-phases of the cell cycle. The EdU label marks cells which synthesized DNA 3 hours before the BrdU injection. Hence, by examining the EdU-labelled cells in the BrdU vs. 7AAD diagram, we introduce a time factor into the cell cycle analysis of the studied cells.

A proportion of the G0/G1-phase cells in the gate 1 was EdU$^+$. These cells originated from the mitotic division of the cells that synthesized DNA before 3 hours (and were either from gate 0 or gate 1). The cells from gate 1 which were in the S-phase (BrdU$^+$) contained two EdU$^+$ cell fractions that were clearly distinguishable by their low or a high DNA content. The EdU$^+$ cells with DNA content close to 2n (in the early S-phase) synthesized DNA 3 hours earlier in the previous cell cycle, mitotically divided and initiated a new round of DNA synthesis in the next cell cycle. The EdU$^+$ cells with the DNA content close to 4n (in the late S-phase) incorporated EdU 3 hours earlier and were still in the S-phase after 3 hours when BrdU was administered. The EdU$^-$ cells in the G1/G0- and S-phases show the cells which did not synthesize DNA when EdU was available, i.e. these cells were in the G2/M- or G1- phases of the cell cycle (Figure

17B). S-phase ($BrdU^+$) cells with a low level of EdU labelling entered the S-phase after EdU administration when EdU was already exhausted and no more was available.

We similarly analysed cells in gates 2 – 4. This revealed that all G1-phase cells (2n) were EdU^+ in these cell populations. This demonstrates that the transition of cells from gate 1 into gate 2 and 3, characterized by a further significant increase in the expression of CD71, is accompanied by cell division. The S-phase cells in gates 2 and 3 consisted predominantly of the cells which incorporated EdU 3 hours earlier in the S-phase of the previous cell cycle. The cells in gate 4 are synchronized in the middle and late parts of the S-phase (see Figure 17B). They contain a few EdU^+ cells which incorporated EdU 3 hours earlier. These cells still synthesized DNA when BrdU was administered, which means that the S-phase lasts >3 hours. The analysis of cells from gates 2 - 4 thus demonstrates that (1) the transition of cells from gate 1 to gates 2/3 requires cell division and (2) that the S-phase to next S-phase transition only takes ≈ 2 hours (or even less because a significant portion of S-phase cells from the previous cell cycle and the next cell cycle overlap, although the time interval between EdU and BrdU administration was only 3 hours), (3) the significant transition in the cell immunuphenotype occurring in gates 2 - 4 takes place in the course of a single S-phase (Figure 17D).

To further extend our dynamic cell cycle analysis, we blocked the mitotic division with colchicine, an inhibitor of microtubule polymerization, which arrests cells in metaphase during their mitotic division (TAYLOR, 1965). Colchicine (0.05 mg/mouse) was given 0.5 hours before the EdU injection which was then followed, after 3 hours, by BrdU injection (Figure 17A). The administration of colchicine resulted in a disruption of erythroid differentiation in $c\text{-}Kit^+$ and CD71 highly positive cells, thus in cells intensively proliferating (Figure 17C). Figure 17B shows the accumulation of 4n cells in the G2/M-phase, in gates 1 and 4. Importantly, the interruption of the influx of EdU^+ cells into the next S-phase in gates 2 and 3 strongly supports our finding that a cell division is required for the transition of cells from gate 1 to gates 2 and 3.

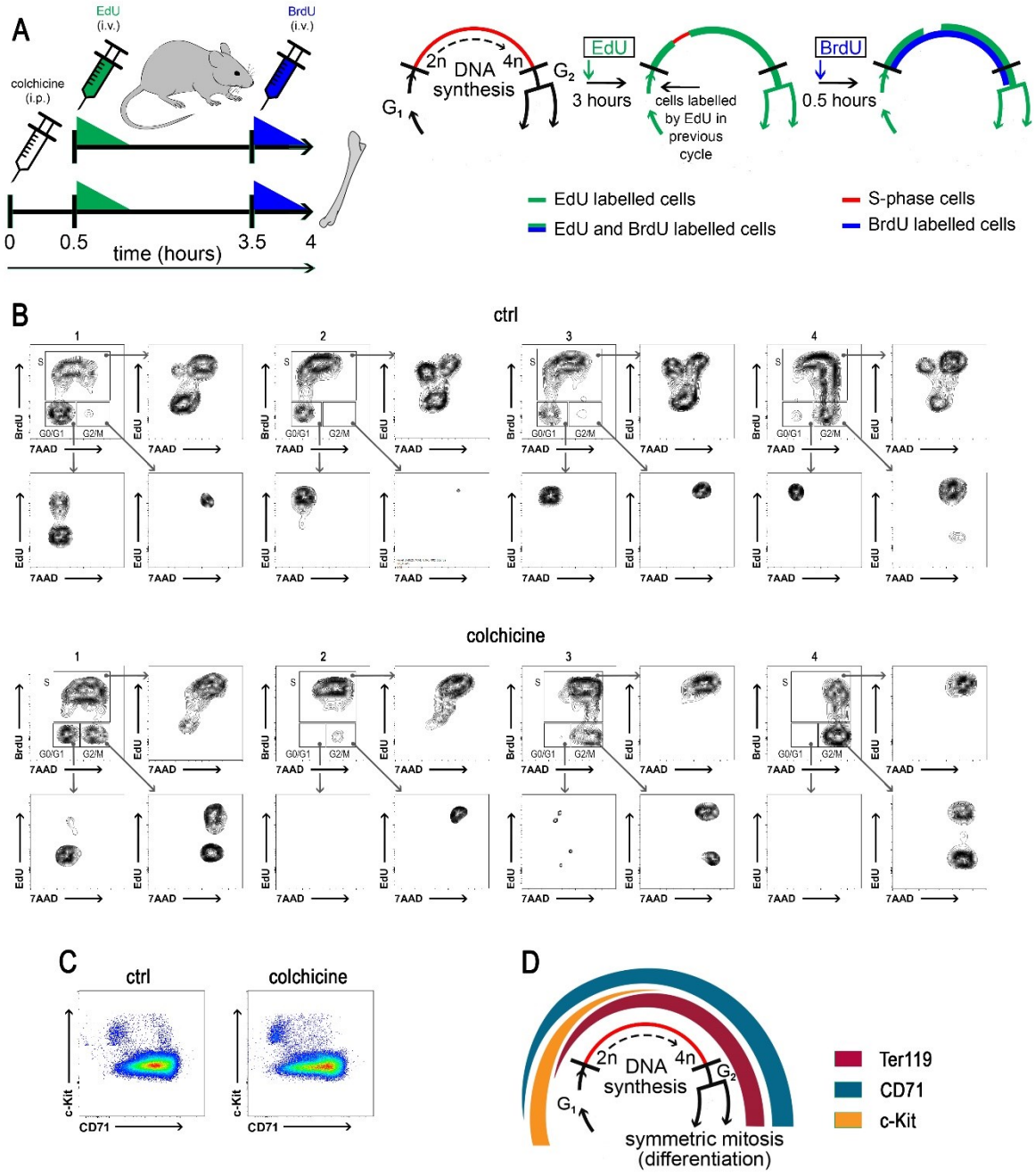

Figure 17 - Dynamic cell cycle analysis of erythroid progenitor and precursor cells in control and colchicine-treated mice

A) *0.5 hours after colchicine administration (0.05 mg/mouse) dual-deoxynucleoside labelling was performed with a single EdU (1.5 mg/mouse) and single BrdU dose (2 mg/mouse) separated by 3 hours. Bone marrow cells were harvested 0.5 hours after the administration of BrdU. Green and blue triangles illustrate the short-term pulse character (approx. 0.5 hours) of EdU and BrdU labelling. A schematic image showing the principle of EdU and BrdU labelling used in this experimental setting is shown on the right.*

B) *Cells from gates 1 - 4 of B220$^-$/Gr-1$^-$/Mac-1$^-$/Sca-1$^-$/CD16_32$^-$ bone marrow cells of control and colchicine-treated mice were plotted on the BrdU vs 7AAD diagram and cell-cycle phases were discriminated. The EdU incorporation was further analysed in cells separated into individual cell-cycle phases.*

C) *Representative examples of B220$^-$/Gr-1$^-$/Mac-1$^-$/Sca-1$^-$/CD16_32$^-$ bone marrow cells of control and colchicine-treated mice.*

D) *Erythroid differentiation steps after mitotic division of cells in population 1 occur during single cell cycle in cells from gates 2 – 4.*

5 Discussion

5.1 Cell cycle and cell cycle kinetics of HSPCs

Haematopoietic tissue is characterized by intensive cell proliferation, resulting in the lifelong production of mature blood cells. The longevity of blood cell production is due to the presence of HSCs possessing both self-renewal and differentiation multilineage developmental potential. However, HSCs in the bone marrow of adult mice divide very rarely (Wilson *et al.*, 2007; Foudi *et al.*, 2009; van der Wath *et al.*, 2009). Therefore, HSCs are linked to blood cell production through actively proliferating progenitor cells. We attempted to estimate the quantitative contribution of various types of these immature haematopoietic cells to steady-state murine haematopoiesis. Although the proliferation rate of these cells has been characterized previously (Passegué *et al.*, 2005; Foudi *et al.*, 2009), the available data were insufficient for estimating the number of cells produced, because this requires knowledge of the rate with which cells divide. We decided to fill this gap in current knowledge by determining the cell flow rates at which various types of immature haematopoietic cells progress through the cell cycle. These enabled us to determine the duration of the S-phase and to calculate the average cell cycle time in LSK cells and in three subtypes of $LS^{-}K$ cells: CMPs, GMPs and MEPs.

To achieve this goal, we first had to optimize the sequential dual labelling of DNA synthesizing cells. We noticed that when bone marrow cells were labelled with a single dose of EdU and a single dose of BrdU separated by 2 hours and collected 0.5 hours after BrdU administration (Figure 8A), the fraction of the cells labelled only with BrdU almost equaled that of cells labelled only with EdU. This strongly suggested that the period when cells incorporated EdU was shorter than the two-hour period preceding BrdU administration. We concluded that the short EdU labelling period led to an underestimation of the fraction of $EdU^{+}BrdU^{+}$ cells, because some cells had started DNA synthesis when EdU was no longer available. We resolved this issue by adding a second EdU injection 0.5 hours before BrdU injection. BrdU is preferentially incorporated into the DNA in the presence of EdU (Bradford and Clarke, 2011), and therefore only a negligible amount of EdU could have been incorporated after BrdU administration in our experiments. However, even if EdU had continued to be incorporated into DNA-synthesizing cells in parallel with BrdU, this would have overestimated the

double-labelled fraction of EdU^+BrdU^+ cells very little as the 0.5h interval is much shorter than the total duration of the S-phase, which is several hours.

Further, we were concerned with the possibility that some EdU^+BrdU^- cells which exited from the S-phase after the first dose of EdU could have divided within two and half hours, thereby artificially increasing the number of EdU^+BrdU^- cells. Therefore, we determined the ratio of EdU^+BrdU^- to EdU^-BrdU^+ cells and compared it with a theoretical ratio corresponding to equal labelling periods for EdU and BrdU. The results of this comparison suggested that a portion of the EdU^+BrdU^- cells indeed could have divided. Therefore, we shortened the interval between the first EdU injection and the BrdU injection to 1.5 hours, which suppressed this distortion.

The recently published study by Akinduro et al. (2018) used dual sequential EdU-BrdU labelling to determine the flow rate of cells entering the S-phase, i.e. the EdU^-BrdU^+ fraction. This study assumed that EdU was available for DNA synthesis for only ≈ 0.5 hours after its administration, which is consistent with our findings. Importantly, the proportion of LSK cells entering the S-phase determined in the Akinduro study (1-3.5 % per hour), was similar to the flow rate of cells exiting the S-phase that we measured (2.2 % per hour), further confirming our results.

After establishing the number of HSPCs leaving the S-phase and entering the G2-phase of the cell cycle, we decided to check the obtained values by independently determining the number of daughter cells arising from their mitotic division. Previous results indicated that 4n cells entering the G2-phase started to divide approximately 1.5 hours later, which resulted in a reduction of their DNA content to 2n. Their number should have doubled if both daughter cells had maintained the phenotype of the mother cell. The DNA content being reduced from 4n to 2n values enabled their clear distinction by flow cytometry. Therefore, we measured the increment of cells with 2n DNA content labelled with BrdU during the preceding S-phase.

The obtained experimental results significantly differed from the expectation that both daughter cells arising from mitosis would maintain the phenotype of the mother cell. Furthermore, they differed in the opposite ways in LSK and LS^-K cells. While newly-produced 2n LSK cells were only 1.1 times their cell flow into the G2-phase, there were seemingly more than 2.0 times in newly-produced LS^-K cells. Neither of the values fitted the model of one cell giving rise to two identical daughter cells during its division. Almost one half of the total progeny of LSK cells lost the LSK phenotype, which strongly suggested that they differentiated

in mitosis. Moreover, there must have been an external source of influx of 2n LS^-K cells in addition to their generation by their own cell division. This led us to formulate a model in which LSK cells self-renew and differentiate into LS^-K cells by predominantly asymmetric cell divisions (Figure 14A).

The resulting ratio of the 2n $BrdU^+$ cell flow rate into the G1-phase and the EdU^+BrdU^- cell flow rate into the G2-phase in LS^-K cells exceeding the theoretical value of 2.0, corresponding to the mitotic doubling effect, was the major challenge in interpretation and understanding our experimental data. This comprise CMPs, GMPs and MEPs. We tentatively attributed this phenomenon to the influx of cells from the LSK cell compartment into LS-K cells. However, in the hierarchical model of haematopoiesis, this influx should only affect CMPs but not GMPs and MEPs. The influx of cells from the LSK population, arising from asymmetric mitosis (Figure 14A), into the G1-phase of CMPs could explain the theoretical value 2.0 being exceeded for CMPs. Therefore, the theoretical value 2.0 being exceeded for GMPs and MEPs still needed to be explained. These cells could receive a similar cell influx from amplified CMPs to the influx into CMPs from differentiated LSK. Another or an additional explanation could be the differentiation of GMPs and MEPs during the S-phase. This differentiation would diminish the cell flow rate into the G2-phase. The distorted ratio of G1/G2 flow rates can also lead to values > 2.0. In this regard, it is important that Pop et al. (2010) and Hwang et al. (2017) demonstrated that in the foetal liver, immature haematopoietic cells achieve the erythroid phenotype during the S-phase of the cell cycle.

Our research, designed primarily to establish the quantitative cell production in various types of haematopoietic progenitor cells, has achieved this goal, as summarized in Figure 14B. It confirmed the role of LS^-K cells in the main amplification stage in the production of blood cells. It also resulted in the refinement of the labelling methods, enabling analysis of the cell cycle characteristics of haematopoietic cells *in vivo*. Unexpectedly, it revealed the significant difference in how the $Sca\text{-}1^+$ and $Sca\text{-}1^-$ subsets of immature haematopoietic cells self-renew and differentiate. This novel discovery points to the specific roles of these two hierarchically linked cell types in haematopoiesis. While the LSK cells maintain their population size and differentiate to LS^-K cells by asymmetric cell divisions, the LS^-K cells primarily amplify their numbers by symmetric self-renewing cell divisions to provide cells that are capable of further

differentiation under local and external cues reflecting immediate needs for specific blood cell types.

5.2 Erythroid developmental pathway in mouse bone marrow analysed by flow cytometry

Identifying the differentiation stages of erythroid progenitor and precursor cells by flow cytometry generally utilizes the cell surface markers CD71 (transferrin receptor 1) and Ter119 (Koulnis *et al.*, 2011). This approach was used by Pop and co-workers for studying erythropoietic differentiation in the foetal liver (Pop *et al.*, 2010; Hwang *et al.*, 2017). In the foetal liver, the CD71/Ter119 cell expression pattern makes it possible to discriminate the cell populations containing early stages of erythroid progenitors with the BFU-E and CFU-E colony-forming potential and the cell populations containing morphologically distinguishable erythroid precursor cells (Pop *et al.*, 2010). In the bone marrow, the cell distribution in the CD71/Ter119 diagram does not fully correspond to the cell distribution in the foetal liver, in particular cells containing the early erythroid progenitor with the BFU-E and CFU-E colony-forming potential cannot be clearly discriminated from other cells.

Therefore, we devised a new approach for the identification and analysis of the erythroid developmental pathway in the bone marrow of adult mice. Instead of the CD71/Ter119 cells profiling that is effective in the foetal liver, we utilised the c-Kit/CD71 profiling in bone marrow cells lacking granulocytes and macrophages (Gr-1 and Mac-1expressing cells) and granulocyte-macrophage progenitors (CD16_32 expressing cells), B-lymphocytes (B220 expressing cells) and Sca-1 expressing immature HSPCs (Figure 15A). This approach enabled us to follow the development of c-Kit^{+}Sca-1^{-}CD71^{-} cells (gate 0) with the highest BFU-E colony-forming potential into the c-Kit^{+}Sca-1^{-}CD71^{medium} cells (gate 1) cells with the highest CFU-E colony-forming potential and further into cells which initiate the expression of the erythroid marker Ter119 (gates 2 - 8) and which no longer give rise to colonies of erythroid cells in a semisolid culture media (Figure 15B).

We used the imaging flow cytometry to characterize the cells plotted in the c-Kit/CD71 diagram with respect to their morphology corresponding to various developmental stages of erythroid precursor cells as developed by McGrath et al. (2008). The imaging flow cytometry combines the FACS analysis with the fluorescent microscopy and enables us to examine much higher cell numbers than traditional microscopic examination. We show that cells in gate 2 correspond to proerythroblasts, cells in gate 4 correspond to basophilic erythroblasts, cells in gate 5 to basophilic and polychromatophilic erythroblasts, and gate 8 contains orthochromatic

erythroblasts and pyrenocytes (extruded nuclei). The erythroid maturing of cells in the gates 5 - 8 is characterized by decreasing CD71 expression in c-Kit$^-$ cells (Figure 15C, D, E).

The analysis of the cell cycle in immature Sca-1 positive HSPCs and in their Sca-1 negative progeny suggested that while Sca-1 positive cells lose the Sca-1 antigen during mitosis, Sca-1 negative cells differentiate in the course of the cell cycle (part 4.2 of this thesis, (Páral *et al.*, 2018)). Therefore, we decided to analyse how Sca-1 negative myeloid progenitors initiate differentiation into erythroid progenitors and red blood cell precursor cells. We chose the erythroid differentiation cell lineage because it is quantitatively important (Necas *et al.*, 1995; Boyer *et al.*, 2019) and analytical tools suitable for its flow cytometry analysis are available. Moreover, Pop et al. (2010) reported that in the foetal liver erythroid differentiation is induced during the S-phase of the cell cycle, when cells reduplicate their genetic material.

To focus upon erythroid cells, we analysed the cell cycle status in B220$^-$/Gr-1$^-$/Mac-1$^-$/Sca-1$^-$/CD16_32$^-$ bone marrow cells. We followed the early erythroid developmental pathway in a c-Kit/CD71 diagram which we evaluated as more sensitive than the traditional CD71/Ter119 diagram in terms of illustrating the very early stages of erythroid cell commitment. The early erythroid differentiation was marked by a distinct increase in CD71 expression in cells expressing high levels of c-Kit. Determination of the cell cycle status of these cells revealed a significant increase in the proliferation rate, indicated by increased incorporation of the DNA precursor BrdU. This index of cell proliferation increased to ≈ 90%, which suggested cell synchronization in the S-phase in gates 2 - 4 (Figure 16C). These results indicate that the early erythroid differentiation is connected with the induction of intensive cell proliferation and with DNA synthesis in the S-phase of the cell cycle. These findings are consistent with erythroid differentiation in the foetal liver, where the up-regulation of CD71 coincides with the synchronization of the last generation of CFU-E cells in the S-phase that is necessary for their further differentiation into proerythroblasts (Pop *et al.*, 2010).

Our results also demonstrate that the differentiation of proerythroblasts (cells in gate 2) into basophilic erythroblasts (cells in gate 4) occurs during the S-phase within a single cell cycle. Moreover, our results revealed that this differentiation step is accompanied by a steep down-regulation of the c-Kit receptor in the early and middle parts of the S-phase (gates 2 and 3). Cells in the early part of the S-phase (gate 2) also exhibited the Ter119 antigen, a hallmark of erythroid cells in their flow cytometry analysis.

To analyse the early phases of erythroid differentiation taking place in c-Kit positive cells in more detail and to introduce a dynamic factor into our analysis, we applied the dual sequential labelling method of DNA synthesizing cells with EdU and BrdU. The time interval separating EdU and BrdU administration enabled us to follow the fate of the cells that were in the late S-phase during EdU administration. We wanted to determine in what part of the cell cycle these cells (EdU^+) will be in three hours later when the cells were labelled with BrdU. This showed that during these three hours the cells which were in the late S-phase mitotically divided and, importantly, a significant part of them initiated a new round of DNA synthesis in the early phase of the S-phase of the next cell cycle (Figure 17 A, B).

We analysed cells labelled with EdU according to their DNA content. This distinguished between cells which were in the early phase of the S-phase with DNA content close to 2n and cells with DNA content close to 4n (in late S-phase), which had incorporated EdU when it was administered and were still in the S-phase of the same cell cycle three hours later. The EdU-labelled cells with DNA content close to 2n and those with DNA content close to 4n were separated by EdU unlabelled cells (Figure 17B). Clearly, these cells entered the S-phase with a delay after EdU administration when EdU was no longer available due to its exhaustion within 0.5 - 1 hour. There were significant differences in this general picture in cells from different gates. Cells in gates 2 and 3 contained a significant fraction of EdU^-labelled cells that started a new round of DNA synthesis within three hours, while cells in the gate 4 predominantly contained EdU labelled cells that were in the early S-phase during EdU administration and after three hours they still synthesized DNA in the final part of the same S-phase. These results confirm our previous conclusion that the cells that undergo significant phenotypic development between gate 2 and gate 4 perform these changes in parallel with the replication of their genetic material (in the S-phase of a single cell cycle).

All G1 cells in gates 2 and 3 were labelled with EdU. From this we conclude that all cells that entered into gate 2 originated in gate 1 and underwent mitotic division connected with their transition into gate 2. The possibility that cells from gate 4 enter a new round of cell division is unlikely, because this would have to be associated with a c-Kit re-expression and with a partial loss of Ter119. Cells from gate 4 thus divide by the symmetric differentiating mitosis and proceed to the next phase of erythroid development as cells completely lacking the c-Kit receptor.

Our results show that a high proportion of CD71 erythroid progenitors synthesize DNA and that the time interval from the S-phase to the S-phase in the next cell cycle may be significantly shorter than 2 hours (part 4.3.3 of this thesis). Such cell cycle properties severely limit the applicability of the dual-pulse sequential labelling of DNA with EdU and BrdU for determining of cell flow rate from the S-phase into the G2-phase as it was described by Páral *et al.* (2018, 2019). Therefore we used colchicine, a drug that arrests cells in the metaphase during mitosis and thus interrupts cell division and the initiation of the next cell cycle, to further enhance this dynamic approach to the cell cycle analysis in erythroid progenitor cells.

The mitotic block lasting 3.5 hours induced by colchicine led to the accumulation of 4n cells in gate 1 and abolished the appearance of EdU^+ cells in gates 2 and 3. This treatment also interfered with the erythroid differentiation exemplified by the augmentation of the CD71 expression occurring between cells in gate 1 and gates 2 and 3 (Figure 17B, C). This further demonstrates that the early phase of the erythroid differentiation is tightly linked with their progression through the cell cycle and, particularly, with the reduplication of the cell genetic material in the S-phase of the cell cycle.

6 Conclusions

The present study provides experimental evidence that

- the fraction of DNA-synthesizing cells is a characteristic feature of various types of HSPCs

- the double-pulse DNA labelling with EdU and BrdU requires optimization for *in vivo* use, then it represents a convenient tool for determining the cell cycle kinetic parameters

- the LSK cells maintain their population size and differentiate to $LS^{-}K$ cells by asymmetric cell divisions

- the $LS^{-}K$ cells primarily amplify their numbers by symmetric self-renewing cell divisions

- the immunophenotypic identification based on c-Kit/CD71 profiling enables to investigate the development of erythroid progenitors into differentiated precursors of red blood cells

- the differentiation of proerythroblasts into basophilic erythroblasts occurs during S-phase within a single cell cycle

7 Summary

Haematopoietic stem and progenitor cells (HSPCs) are crucial for lifelong blood cell production. We analysed the cell cycle and cell production rate in HSPCs in murine haematopoiesis. The labelling of DNA-synthesizing cells by two thymidine analogues, optimized for *in-vivo* use, enabled the determination of the cell cycle flow rate into the G2-phase, the duration of the S-phase and the average cell cycle time in Sca-1$^+$ and Sca-1$^-$ HSPCs. The determination of cells with 2n DNA content and labelled during the preceding S-phase was used to establish the cell flow rates in the G1-phase. Our measurements revealed a significant difference in how Sca-1$^+$ and Sca-1$^-$ HSPCs self-renew and differentiate. The division of Sca-1$^+$ progenitors led to the loss of the Sca-1 marker in about half of newly produced cells, corresponding to asymmetric cell division. In contrast both Sca-1$^-$ progenitors, arising from mitotic cell division, entered a new round of the cell cycle. This corresponds to symmetric self-renewing cell division. The novel data also enabled us to estimate the cell production rates in the Sca-1$^+$ and in three subtypes of Sca-1$^-$ HSPCs.

We focused on adult murine erythroid differentiation in the next part of our study. We introduced an original flow cytometry approach for identifying and studying erythroid progenitor and precursor cells. This approach is based on the changing expression of two cell surface markers, c-Kit (receptor for stem cell factor) and CD71 (transferrin receptor 1) in bone marrow cells deprived of granulocytes, monocytes, lymphocytes and Sca-1$^+$ cells. We identified the early erythroid progenitor cells with BFU-E and CFU-E potentials within the cell population highly expressing c-Kit. The potential to give rise to BFU-E and CFU-E colonies was lost in the cells highly expressing CD71. Subsequently, erythroid differentiation progressed into the proerythroblasts which expressed c-Kit at a high level. Analysis of the cell cycle revealed that the differentiation of proerythroblasts into basophilic erythroblasts occurs in the course of a single cell cycle, in fact predominantly in the S-phase. During this S-phase, cells maintain the high expression of CD71 but rapidly lose the c-Kit marker and express the erythroid marker Ter119. The dual EdU-BrdU sequential labelling of DNA synthesizing cells, together with the metaphase block induced by colchicine, provide us with unique insights into the dynamics of cell proliferation and differentiation events in early erythroid cells.

8 Souhrn

Krvetvorné kmenové a progenitorové buňky jsou nezbytné pro celoživotní produkci krevních buněk. Analyzovali jsme buněčný cyklus a intenzitu produkce těchto buněk v myší krvetvorné tkáni. Značení buněk syntetizujících DNA dvěma tymidinovými analogy, optimalizované pro *in vivo* použití, umožnilo stanovit rychlost, s jakou buňky vstupují do G2-fáze buněčného cyklu, výpočet délky trvání S-fáze a průměrné délky buněčného cyklu v Sca-1$^+$ a Sca-1$^-$ subtypech krvetvorných kmenových a progenitorových buněk. Diploidní buňky, které byly označeny v průběhu S-fáze předchozího buněčného cyklu, byly využity pro stanovení rychlosti, se kterou tyto buňky vstupují do G1-fáze buněčného cyklu. Tyto naše analýzy ukázaly významný rozdíl v sebeobnovném a diferenciačním charakteru buněčného dělení Sca-1$^+$ a Sca-1$^-$ buněk. Po rozdělení Sca-1$^+$ buněk asi polovina nově vzniklých buněk ztratila Sca-1, což odpovídá asymetrickému dělení. Oproti tomu, Sca-1$^-$ buňky se dělily sebeobnovným symetrickým dělením. Tyto nové údaje nám dále umožnily odhadnout rychlosti buněčných produkcí v Sca-1$^+$ buňkách a v 3 subtypech Sca-1$^-$ buněk.

V druhé části studie jsme se zaměřili na erytroidní diferenciaci kmenových a progenitorových buněk. Zavedli jsme nový způsob identifikace erytroidních progenitorů a prekurzorů v kostní dřeni a sledování průběhu jejich diferenciace. Tyto analýzy jsou založeny na měnící se expresi dvou povrchových znaků, c-Kit (receptor pro stem cell factor) a CD71 (transferinový receptor 1) na buňkách kostní dřeně, které byly zbaveny granulocytů, monocytů, lymfocytů a Sca-1$^+$ buněk. V buňkách vyznačujících se vysokou expresí c-Kit jsme prokázali časné erytroidní progenitory schopné tvořit kolonie BFU-E a CFU-E. Tato schopnost byla silně snížena v c-Kit$^+$ buňkách s nejvyšší expresí CD71. Na buňky obsahující BFU-E a CFU-E erytroidní progenitory navazuje stadium proerytroblastu, které stále intenzivně exprimuje c-Kit při současné vysoké expresi CD71. Analýzou buněčného cyklu bylo zjištěno, že následná diferenciace proerytroblastů do bazofilních erytroblastů se odehrává v průběhu jediného buněčného cyklu a to převážně v jeho S-fázi. V průběhu této S-fáze buňky udržují vysokou expresi CD71, rychle ztrácejí c-Kit receptor a zvyšují expresi erytroidního znaku Ter119. Metodika dvojitého značení buněk syntetizujících DNA pomocí EdU a BrdU, společně se zastavením buněk v stadiu metafáze kolchicinem, umožnily jedinečný náhled do dynamiky proliferace a diferenciace časných progenitorů a prekurzorů červených krvinek.

9 Key words

haematopoiesis, stem cells, progenitor cells, cell cycle, differentiation, erythropoiesis

10 Klíčová slova

krvetvorba, kmenové buňky, progenitorové buňky, buněčný cyklus, diferenciace, erytropoéza

11 References

Abukhdeir, A. M. and Park, B. H. (2008) 'P21 and p27: roles in carcinogenesis and drug resistance.', *Expert reviews in molecular medicine*. NIH Public Access, 10, p. e19. doi: 10.1017/S1462399408000744.

Acar, M. *et al.* (2015) 'Deep imaging of bone marrow shows non-dividing stem cells are mainly perisinusoidal', *Nature*, 526(7571), pp. 126–130. doi: 10.1038/nature15250.

Adolfsson, J. *et al.* (2001) 'Upregulation of Flt3 expression within the bone marrow Lin(-)Sca1(+)c-kit(+) stem cell compartment is accompanied by loss of self-renewal capacity.', *Immunity*, 15(4), pp. 659–69.

Akashi, K. *et al.* (2000) 'A clonogenic common myeloid progenitor that gives rise to all myeloid lineages.', *Nature*, 404(6774), pp. 193–7. doi: 10.1038/35004599.

Akinduro, O. *et al.* (2018) 'Proliferation dynamics of acute myeloid leukaemia and haematopoietic progenitors competing for bone marrow space', *Nature Communications*, 9(1), p. 519. doi: 10.1038/s41467-017-02376-5.

Arai, F. *et al.* (2004) 'Tie2/Angiopoietin-1 Signaling Regulates Hematopoietic Stem Cell Quiescence in the Bone Marrow Niche', *Cell*, 118(2), pp. 149–161. doi: 10.1016/j.cell.2004.07.004.

Arinobu, Y. *et al.* (2007) 'Reciprocal Activation of GATA-1 and PU.1 Marks Initial Specification of Hematopoietic Stem Cells into Myeloerythroid and Myelolymphoid Lineages', *Cell Stem Cell*, 1(4), pp. 416–427. doi: 10.1016/j.stem.2007.07.004.

Baron, M. H. (2013) 'Concise Review: early embryonic erythropoiesis: not so primitive after all.', *Stem cells (Dayton, Ohio)*. NIH Public Access, 31(5), pp. 849–56. doi: 10.1002/stem.1342.

Baron, M. H., Isern, J. and Fraser, S. T. (2012) 'The embryonic origins of erythropoiesis in mammals.', *Blood*. The American Society of Hematology, 119(21), pp. 4828–37. doi: 10.1182/blood-2012-01-153486.

Berthet, C. *et al.* (2003) 'Cdk2 knockout mice are viable.', *Current biology : CB*, 13(20), pp. 1775–85.

Boyer, S. W. *et al.* (2019) 'Clonal and Quantitative In Vivo Assessment of Hematopoietic Stem Cell Differentiation Reveals Strong Erythroid Potential of Multipotent Cells', *Stem Cell Reports*, 12(4), pp. 801–815. doi: 10.1016/j.stemcr.2019.02.007.

Bradford, J. A. and Clarke, S. T. (2011) 'Dual-Pulse Labeling Using 5-Ethynyl-2'-Deoxyuridine (EdU) and 5-Bromo-2'-Deoxyuridine (BrdU) in Flow Cytometry', in *Current Protocols in Cytometry*. Hoboken, NJ, USA: John Wiley & Sons, Inc., p. Unit 7.38. doi: 10.1002/0471142956.cy0738s55.

Bregman, D. B., Pestell, R. G. and Kidd, V. J. (2000) 'Cell cycle regulation and RNA polymerase II.', *Frontiers in bioscience : a journal and virtual library*, 5, pp. D244-57.

Busch, K. *et al.* (2015) 'Fundamental properties of unperturbed haematopoiesis from stem cells in vivo', *Nature*, 518(7540), pp. 542–546. doi: 10.1038/nature14242.

Cánepa, E. T. *et al.* (2007) 'INK4 proteins, a family of mammalian CDK inhibitors with novel biological functions', *IUBMB Life*, 59(7), pp. 419–426. doi: 10.1080/15216540701488358.

Cantor, A. B. and Orkin, S. H. (2001) 'Hematopoietic development: a balancing act', *Current Opinion in Genetics & Development*. Elsevier Current Trends, 11(5), pp. 513–519. doi: 10.1016/S0959-437X(00)00226-4.

Carrelha, J. *et al.* (2018) 'Hierarchically related lineage-restricted fates of multipotent haematopoietic stem cells', *Nature*, 554(7690), pp. 106–111. doi: 10.1038/nature25455.

Challen, G. A. *et al.* (2009) 'Mouse hematopoietic stem cell identification and analysis', *Cytometry Part A*, 75A(1), pp. 14–24. doi: 10.1002/cyto.a.20674.

Chen, C.-Z. *et al.* (2002) 'Nonlinear partial differential equations and applications: Identification of endoglin as a functional marker that defines long-term repopulating hematopoietic stem cells', *Proceedings of the National Academy of Sciences*, 99(24), pp. 15468–15473. doi: 10.1073/pnas.202614899.

Chen, C.-Z. *et al.* (2003) 'The endoglin(positive) sca-1(positive) rhodamine(low) phenotype defines a near-homogeneous population of long-term repopulating hematopoietic stem cells.', *Immunity*, 19(4), pp. 525–33.

Chen, K. *et al.* (2009) 'Resolving the distinct stages in erythroid differentiation based on dynamic changes in membrane protein expression during erythropoiesis.', *Proceedings of the National Academy of Sciences of the United States of America*. National Academy of Sciences, 106(41), pp. 17413–8. doi: 10.1073/pnas.0909296106.

Clurman, B. E. *et al.* (1996) 'Turnover of cyclin E by the ubiquitin-proteasome pathway is regulated by cdk2 binding and cyclin phosphorylation.', *Genes & development*, 10(16), pp. 1979–90.

Cobrinik, D. (2005) 'Pocket proteins and cell cycle control', *Oncogene*, 24(17), pp. 2796–2809. doi: 10.1038/sj.onc.1208619.

Coverley, D., Laman, H. and Laskey, R. A. (2002) 'Distinct roles for cyclins E and A during DNA replication complex assembly and activation', *Nature Cell Biology*, 4(7), pp. 523–528. doi: 10.1038/ncb813.

Cukier, I. H., Li, Y. and Lee, J. M. (2007) 'Cyclin B1/Cdk1 binds and phosphorylates Filamin A and regulates its ability to cross-link actin', *FEBS Letters*, 581(8), pp. 1661–1672. doi: 10.1016/j.febslet.2007.03.041.

Dai, C. H., Krantz, S. B. and Zsebo, K. M. (1991) 'Human burst-forming units-erythroid need direct interaction with stem cell factor for further development.', *Blood*, 78(10), pp. 2493–7.

Davidson, G. *et al.* (2009) 'Cell Cycle Control of Wnt Receptor Activation', *Developmental Cell*, 17(6), pp. 788–799. doi: 10.1016/j.devcel.2009.11.006.

Dumitru, A. M. G. *et al.* (2017) 'Cyclin A/Cdk1 modulates Plk1 activity in prometaphase to regulate kinetochore-microtubule attachment stability', *eLife*, 6. doi: 10.7554/eLife.29303.

Dzierzak, E. and Philipsen, S. (2013) 'Erythropoiesis: Development and Differentiation', *Cold Spring Harbor Perspectives in Medicine*, 3(4), pp. a011601–a011601. doi: 10.1101/cshperspect.a011601.

Elliott, S., Pham, E. and Macdougall, I. C. (2008) 'Erythropoietins: A common mechanism of action', *Experimental Hematology*. Elsevier, 36(12), pp. 1573–1584. doi: 10.1016/J.EXPHEM.2008.08.003.

den Elzen, N. and Pines, J. (2001) 'Cyclin A is destroyed in prometaphase and can delay chromosome alignment and anaphase.', *The Journal of cell biology*, 153(1), pp. 121–36.

Forgacova, K. *et al.* (2013) 'All hematopoietic stem cells engraft in submyeloablatively irradiated mice', *Biology of Blood and Marrow Transplantation*, 19(5), pp. 713–719. doi: 10.1016/j.bbmt.2013.02.012.

Forsberg, E. C. *et al.* (2005) 'Differential Expression of Novel Potential Regulators in Hematopoietic Stem Cells', *PLoS Genetics*, 1(3), p. e28. doi: 10.1371/journal.pgen.0010028.

Foudi, A. *et al.* (2009) 'Analysis of histone 2B-GFP retention reveals slowly cycling hematopoietic stem cells.', *Nature biotechnology*, 27(1), pp. 84–90. doi: 10.1038/nbt.1517.

Fung, T. K., Ma, H. T. and Poon, R. Y. C. (2007) 'Specialized Roles of the Two Mitotic Cyclins in Somatic Cells: Cyclin A as an Activator of M Phase-promoting Factor', *Molecular Biology of the Cell*, 18(5), pp. 1861–1873. doi: 10.1091/mbc.E06-12-1092.

Geley, S. *et al.* (2001) 'Anaphase-promoting complex/cyclosome-dependent proteolysis of human cyclin A starts at the beginning of mitosis and is not subject to the spindle assembly checkpoint.', *The Journal of cell biology*, 153(1), pp. 137–48.

Gonchoroff, N. J. *et al.* (1985) 'A monoclonal antibody reactive with 5-bromo-2-deoxyuridine that does not require DNA denaturation', *Cytometry*, 6(6), pp. 506–512. doi: 10.1002/cyto.990060604.

Gonchoroff, N. J. *et al.* (1986) 'S-phase detection with an antibody to bromodeoxyuridine. Role of DNase pretreatment.', *Journal of immunological methods*, 93(1), pp. 97–101.

Goodell, M. A. *et al.* (1996) 'Isolation and functional properties of murine hematopoietic stem cells that are replicating in vivo.', *The Journal of experimental medicine*. The Rockefeller University Press, 183(4), pp. 1797–806.

Gregory, C. J. and Eaves, A. C. (1978) 'Three stages of erythropoietic progenitor cell differentiation distinguished by a number of physical and biologic properties.', *Blood*, 51(3), pp. 527–37.

Grover, A. *et al.* (2014) 'Erythropoietin guides multipotent hematopoietic progenitor cells toward an erythroid fate', *Journal of Experimental Medicine*. Rockefeller University Press, 211(2), pp. 181–188. doi: 10.1084/JEM.20131189.

Hagting, A. *et al.* (2002) 'Human securin proteolysis is controlled by the spindle checkpoint and reveals when the APC/C switches from activation by Cdc20 to Cdh1', *The Journal of Cell Biology*, 157(7), pp. 1125–1137. doi: 10.1083/jcb.200111001.

Hinds, P. W. *et al.* (1992) 'Regulation of retinoblastoma protein functions by ectopic expression of human cyclins.', *Cell*, 70(6), pp. 993–1006.

Hoppe, P. S. *et al.* (2016) 'Early myeloid lineage choice is not initiated by random PU.1 to GATA1 protein ratios', *Nature*, 535(7611), pp. 299–302. doi: 10.1038/nature18320.

Horton, L. E. and Templeton, D. J. (1997) 'The cyclin box and C-terminus of cyclins A and E specify CDK activation and substrate specificity', *Oncogene*, 14(4), pp. 491–498. doi: 10.1038/sj.onc.1200851.

Howard, A. & Pelc, S.R., (1953) Synthesis of Deoxyribonucleic Acid in Normal and Irradiated Cells and Its Relation to Chromosome Breakage. *Heredity* 6 (suppl.), 261-273.

Hwang, Y. *et al.* (2017) 'Global increase in replication fork speed during a p57KIP2-regulated erythroid cell fate switch', *Science Advances*. American Association for the Advancement of Science, 3(5), p. e1700298. doi: 10.1126/sciadv.1700298.

Ikuta, K. and Weissman, I. L. (1992) 'Evidence that hematopoietic stem cells express mouse c-kit but do not depend on steel factor for their generation.', *Proceedings of the National Academy of Sciences of the United States of America*. National Academy of Sciences, 89(4), pp. 1502–6.

Ivanovska, I. *et al.* (2008) 'MicroRNAs in the miR-106b family regulate p21/CDKN1A and promote cell cycle progression.', *Molecular and cellular biology*. American Society for Microbiology (ASM), 28(7), pp. 2167–74. doi: 10.1128/MCB.01977-07.

Johnson, A. and Skotheim, J. M. (2013) 'Start and the restriction point', *Current Opinion in Cell Biology*, 25(6), pp. 717–723. doi: 10.1016/j.ceb.2013.07.010.

Kabeche, L. and Compton, D. A. (2013) 'Cyclin A regulates kinetochore microtubules to promote faithful chromosome segregation', *Nature*, 502(7469), pp. 110–113. doi: 10.1038/nature12507.

Kadri, Z. *et al.* (2009) 'Direct Binding of pRb/E2F-2 to GATA-1 Regulates Maturation and Terminal Cell Division during Erythropoiesis', *PLoS Biology*. Edited by M. A. Goodell. Public Library of Science, 7(6), p. e1000123. doi: 10.1371/journal.pbio.1000123.

Kadri, Z. *et al.* (2015) 'Erythropoietin and IGF-1 signaling synchronize cell proliferation and maturation during erythropoiesis.', *Genes & development*. Cold Spring Harbor Laboratory Press, 29(24), pp. 2603–16. doi: 10.1101/gad.267633.115.

Kang, L. *et al.* (2013) 'Characterization and ex vivo Expansion of Human Placenta-Derived Natural Killer Cells for Cancer Immunotherapy.', *Frontiers in immunology*. Frontiers Media SA, 4, p. 101. doi: 10.3389/fimmu.2013.00101.

Kannourakis, G. and Johnson, G. R. (1988) 'Fractionation of subsets of BFU-E from normal human bone marrow: responsiveness to erythropoietin, human placental-conditioned medium, or granulocyte-macrophage colony-stimulating factor.', *Blood*, 71(3), pp. 758–65.

Kiel, M. J. *et al.* (2005) 'SLAM family receptors distinguish hematopoietic stem and progenitor cells and reveal endothelial niches for stem cells.', *Cell*, 121(7), pp. 1109–21. doi: 10.1016/j.cell.2005.05.026.

Kina, T. *et al.* (2000) 'The monoclonal antibody TER-119 recognizes a molecule associated with glycophorin A and specifically marks the late stages of murine erythroid lineage.', *British journal of haematology*, 109(2), pp. 280–7.

Kishimoto, T. (2015) 'Entry into mitosis: a solution to the decades-long enigma of MPF', *Chromosoma*, 124(4), pp. 417–428. doi: 10.1007/s00412-015-0508-y.

Kondo, M., Weissman, I. L. and Akashi, K. (1997) 'Identification of clonogenic common lymphoid progenitors in mouse bone marrow.', *Cell*, 91(5), pp. 661–72.

Koulnis, M. *et al.* (2011) 'Identification and Analysis of Mouse Erythroid Progenitors using the CD71/TER119 Flow-cytometric Assay', *Journal of Visualized Experiments*, (54). doi: 10.3791/2809.

Lewis, J. L. *et al.* (1998) 'INTERLEUKIN 3 (IL-3), BUT NOT STEM CELL FACTOR (SCF) INCREASES SELF-RENEWAL BY HUMAN ERYTHROID BURST-FORMING UNITS (BFU-E) IN VITRO', *Cytokine*, 10(1), pp. 49–54. doi: 10.1006/cyto.1997.0256.

Liboska, R. *et al.* (2012) 'Most Anti-BrdU Antibodies React with 2'-Deoxy-5-Ethynyluridine — The Method for the Effective Suppression of This Cross-Reactivity', *PLoS ONE*. Edited by B. G. Vertessy, 7(12), p. e51679. doi: 10.1371/journal.pone.0051679.

Lok, C. N. and Ponka, P. (2000) 'Identification of an Erythroid Active Element in the Transferrin Receptor Gene', *Journal of Biological Chemistry*, 275(31), pp. 24185–24190. doi: 10.1074/jbc.M000944200.

Ma, Z. *et al.* (2013) 'Phylogenetic analysis reveals the evolution and diversification of cyclins in eukaryotes', *Molecular Phylogenetics and Evolution*, 66(3), pp. 1002–1010. doi: 10.1016/j.ympev.2012.12.007.

Malumbres, M. *et al.* (2004) 'Mammalian Cells Cycle without the D-Type Cyclin-Dependent Kinases Cdk4 and Cdk6', *Cell*, 118(4), pp. 493–504. doi: 10.1016/j.cell.2004.08.002.

Malumbres, M. (2014) 'Cyclin-dependent kinases.', *Genome biology*, 15(6), p. 122.

Malumbres, M. and Barbacid, M. (2005) 'Mammalian cyclin-dependent kinases', *Trends in Biochemical Sciences*, 30(11), pp. 630–641. doi: 10.1016/j.tibs.2005.09.005.

Martynoga, B. *et al.* (2005) 'Foxg1 is required for specification of ventral telencephalon and region-specific regulation of dorsal telencephalic precursor proliferation and apoptosis', *Developmental Biology*, 283(1), pp. 113–127. doi: 10.1016/j.ydbio.2005.04.005.

Massey, A. J. *et al.* (2015) 'Multiparametric Cell Cycle Analysis Using the Operetta High-Content Imager and Harmony Software with PhenoLOGIC', *PLOS ONE*. Edited by S. Cotterill. Public Library of Science, 10(7), p. e0134306. doi: 10.1371/journal.pone.0134306.

McGrath, K. E., Bushnell, T. P. and Palis, J. (2008) 'Multispectral imaging of hematopoietic cells: Where flow meets morphology', *Journal of Immunological Methods*, 336(2), pp. 91–97. doi: 10.1016/j.jim.2008.04.012.

Mcgrath, K. E., Catherman, S. C. and Palis, J. (2017) 'Delineating stages of erythropoiesis using imaging flow cytometry', *Methods*, 112, pp. 68–74. doi: 10.1016/j.ymeth.2016.08.012.

McLeod, D. L., Shreeve, M. M. and Axelrad, A. A. (1974) 'Improved plasma culture system for production of erythrocytic colonies in vitro: quantitative assay method for CFU-E.', *Blood*, 44(4), pp. 517–34.

Metcalf, D. (2008) 'Hematopoietic cytokines', *Blood*, 111(2), pp. 485–491. doi: 10.1182/blood-2007-03-079681.

Moras, M., Lefevre, S. D. and Ostuni, M. A. (2017) 'From Erythroblasts to Mature Red Blood Cells: Organelle Clearance in Mammals', *Frontiers in Physiology*, 8, p. 1076. doi: 10.3389/fphys.2017.01076.

Morgan, D. O. (1997) 'CYCLIN-DEPENDENT KINASES: Engines, Clocks, and Microprocessors', *Annu. Rev. Cell Dev. Biol*, 13, pp. 261–91.

Morita, Y., Ema, H. and Nakauchi, H. (2010) 'Heterogeneity and hierarchy within the most primitive hematopoietic stem cell compartment', *The Journal of Experimental Medicine*, 207(6), pp. 1173–1182. doi: 10.1084/jem.20091318.

Mossadegh-Keller, N. *et al.* (2013) 'M-CSF instructs myeloid lineage fate in single haematopoietic stem cells', *Nature*, 497(7448), pp. 239–243. doi: 10.1038/nature12026.

Muta, K. *et al.* (1994) 'Distinct roles of erythropoietin, insulin-like growth factor I, and stem cell factor in the development of erythroid progenitor cells.', *Journal of Clinical Investigation*, 94(1), pp. 34–43. doi: 10.1172/JCI117327.

Na Nakorn, T. *et al.* (2002) 'Myeloerythroid-restricted progenitors are sufficient to confer radioprotection and provide the majority of day 8 CFU-S.', *The Journal of clinical investigation*, 109(12), pp. 1579–85. doi: 10.1172/JCI15272.

Nakada, D. *et al.* (2014) 'Oestrogen increases haematopoietic stem-cell self-renewal in females and during pregnancy', *Nature*, 505(7484), pp. 555–558. doi: 10.1038/nature12932.

Nakayama, Kei-ichi and Nakayama, Keiko (1999) 'Cip/Kip cyclin-dependent kinase inhibitors: brakes of the cell cycle engine during development', *BioEssays*, 20(12), pp. 1020–1029. doi: 10.1002/(SICI)1521-1878(199812)20:12<1020::AID-BIES8>3.0.CO;2-D.

Necas, E. *et al.* (1995) 'Hematopoietic reserve provided by spleen colony-forming units (CFU-S).', *Experimental hematology*, 23(12), pp. 1242–6.

Nerlov, C. *et al.* (2000) 'GATA-1 interacts with the myeloid PU.1 transcription factor and represses PU.1-dependent transcription.', *Blood*, 95(8), pp. 2543–51.

Nerlov, C. and Graf, T. (1998) 'PU.1 induces myeloid lineage commitment in multipotent hematopoietic progenitors.', *Genes & development*, 12(15), pp. 2403–12.

Nigg, E. A. (2001) 'Mitotic kinases as regulators of cell division and its checkpoints', *Nature Reviews Molecular Cell Biology*, 2(1), pp. 21–32. doi: 10.1038/35048096.

Novak, J. P. and Necas, E. (1994) 'Proliferation-differentiation pathways of murine haemopoiesis: correlation of lineage fluxes', *Cell Proliferation*. Blackwell Publishing Ltd, 27(10), pp. 597–633. doi: 10.1111/j.1365-2184.1994.tb01377.x.

Nowakowski, R. S., Lewin, S. B. and Miller, M. W. (1989) 'Bromodeoxyuridine immunohistochemical determination of the lengths of the cell cycle and the DNA-synthetic phase for an anatomically defined population.', *Journal of neurocytology*, 18(3), pp. 311–8.

Oguro, H., Ding, L. and Morrison, S. J. (2013) 'SLAM family markers resolve functionally distinct subpopulations of hematopoietic stem cells and multipotent progenitors.', *Cell stem cell*, 13(1), pp. 102–16. doi: 10.1016/j.stem.2013.05.014.

Okada, S. *et al.* (1991) 'Enrichment and characterization of murine hematopoietic stem cells that express c-kit molecule.', *Blood*, 78(7), pp. 1706–12.

Orkin, S. H. (2000) 'Diversification of haematopoietic stem cells to specific lineages', *Nature Reviews Genetics*, 1(1), pp. 57–64. doi: 10.1038/35049577.

Palis, J. (2014) 'Primitive and definitive erythropoiesis in mammals.', *Frontiers in physiology*. Frontiers Media SA, 5, p. 3. doi: 10.3389/fphys.2014.00003.

Páral, P. *et al.* (2018) 'Cell cycle and differentiation of Sca-1 $^{+}$ and Sca-1 $^{-}$ hematopoietic stem and progenitor cells', *Cell Cycle*. Taylor & Francis, 17(16), pp. 1979–1991. doi: 10.1080/15384101.2018.1502573.

Páral, P. *et al.* (2019) 'Cell Cycle Analysis Using In Vivo Staining of DNA-Synthesizing Cells.', *Methods in molecular biology (Clifton, N.J.)*. doi: 10.1007/7651_2019_228.

Pardee, A. B. (1974) 'A restriction point for control of normal animal cell proliferation.', *Proceedings of the National Academy of Sciences of the United States of America*, 71(4), pp. 1286–90.

Passegué, E. *et al.* (2005) 'Global analysis of proliferation and cell cycle gene expression in the regulation of hematopoietic stem and progenitor cell fates.', *The Journal of experimental medicine*. Rockefeller University Press, 202(11), pp. 1599–611. doi: 10.1084/jem.20050967.

Piscopo, D. M. and Hinds, P. W. (2008) 'A Role for the Cyclin Box in the Ubiquitin-Mediated Degradation of Cyclin G1', *Cancer Research*, 68(14), pp. 5581–5590. doi: 10.1158/0008-5472.CAN-07-6346.

Pollack, A. *et al.* (1995) 'Specific staining of iododeoxyuridine and bromodeoxyuridine in tumors double labelled in vivo: A cell kinetic analysis', *Cytometry*, 20(1), pp. 53–61. doi: 10.1002/cyto.990200109.

Pop, R. *et al.* (2010) 'A Key Commitment Step in Erythropoiesis Is Synchronized with the Cell Cycle Clock through Mutual Inhibition between PU.1 and S-Phase Progression', *PLoS Biol*, 8(9). doi: 10.1371/journal.pbio.1000484.

Qiu, J. *et al.* (2014) 'Divisional history and hematopoietic stem cell function during homeostasis.', *Stem cell reports*, 2(4), pp. 473–90. doi: 10.1016/j.stemcr.2014.01.016.

Raza, A. *et al.* (1997) 'Cell cycle kinetic studies in 68 patients with myelodysplastic syndromes following intravenous iodo- and/or bromodeoxyuridine.', *Experimental hematology*, 25(6), pp. 530–5.

Ritter, M. A. *et al.* (1994) 'Tumor cell kinetics using two labels and flow cytometry', *Cytometry*, 16(1), pp. 49–58. doi: 10.1002/cyto.990160108.

Salic, A. and Mitchison, T. J. (2008) 'A chemical method for fast and sensitive detection of DNA synthesis in vivo', *Proceedings of the National Academy of Sciences*, 105(7), pp. 2415–2420. doi: 10.1073/pnas.0712168105.

Sanjuan-Pla, A. *et al.* (2013) 'Platelet-biased stem cells reside at the apex of the haematopoietic stem-cell hierarchy', *Nature*, 502(7470), pp. 232–236. doi: 10.1038/nature12495.

Shibui, S. *et al.* (1989) 'Double labeling with iodo- and bromodeoxyuridine for cell kinetics studies.', *Journal of Histochemistry & Cytochemistry*, 37(7), pp. 1007–1011. doi: 10.1177/37.7.2659659.

Siu, K. T., Rosner, M. R. and Minella, A. C. (2012) 'An integrated view of cyclin E function and regulation', *Cell Cycle*, 11(1), pp. 57–64. doi: 10.4161/cc.11.1.18775.

Spangrude, G. J., Heimfeld, S. and Weissman, I. L. (1988) 'Purification and characterization of mouse hematopoietic stem cells.', *Science (New York, N.Y.)*, 241(4861), pp. 58–62.

Stephenson, J. R. *et al.* (1971) 'Induction of colonies of hemoglobin-synthesizing cells by erythropoietin in vitro.', *Proceedings of the National Academy of Sciences of the United States of America*. National Academy of Sciences, 68(7), pp. 1542–6.

Takagi, S. *et al.* (1993) 'Detection of 5-bromo-2-deoxyuridine (BrdUrd) incorporation with monoclonal anti-brdurd antibody after deoxyribonuclease treatment', *Cytometry*, 14(6), pp. 640–648. doi: 10.1002/cyto.990140608.

TAYLOR, E. W. (1965) 'THE MECHANISM OF COLCHICINE INHIBITION OF MITOSIS. I. KINETICS OF INHIBITION AND THE BINDING OF H3-COLCHICINE.', *The Journal of cell biology*, 25, p. SUPPL:145-60.

Tsang, A. P. *et al.* (1997) 'FOG, a multitype zinc finger protein, acts as a cofactor for transcription factor GATA-1 in erythroid and megakaryocytic differentiation.', *Cell*, 90(1), pp. 109–19.

Udroiu, I. (2016) 'Development of Erythropoiesis in the Mouse 1', *Russian Journal of Developmental Biology*. Pleiades Publishing, Inc, 47(5), pp. 254–259. doi: 10.1134/S1062360416050052.

Vanderlaan, M. *et al.* (1986) 'Improved High-Minity Monoclonal Antibody to Iododeoxyuridinel?'', *Cytometry*, 7, pp. 499–507.

van der Wath, R. C. *et al.* (2009) 'Estimating Dormant and Active Hematopoietic Stem Cell Kinetics through Extensive Modeling of Bromodeoxyuridine Label-Retaining Cell Dynamics', *PLoS ONE*. Edited by A. Leri, 4(9), p. e6972. doi: 10.1371/journal.pone.0006972.

Weksberg, D. C. *et al.* (2008) 'CD150- side population cells represent a functionally distinct population of long-term hematopoietic stem cells', *Blood*, 111(4), pp. 2444–2451. doi: 10.1182/blood-2007-09-115006.

Welschinger, R. and Bendall, L. J. (2015) 'Temporal Tracking of Cell Cycle Progression Using Flow Cytometry without the Need for Synchronization.', *Journal of visualized experiments : JoVE*. MyJoVE Corporation, (102), p. e52840. doi: 10.3791/52840.

Wilson, A. *et al.* (2007) 'Dormant and self-renewing hematopoietic stem cells and their niches.', *Annals of the New York Academy of Sciences*, 1106, pp. 64–75. doi: 10.1196/annals.1392.021.

Wilson, A. *et al.* (2008) 'Hematopoietic Stem Cells Reversibly Switch from Dormancy to Self-Renewal during Homeostasis and Repair', *Cell*, 135(6), pp. 1118–1129. doi: 10.1016/j.cell.2008.10.048.

Woo, R. A. and Poon, R. Y. C. (2003) 'Cyclin-Dependent Kinases and S Phase Control in Mammalian Cells', *Cell Cycle*, 2(4), pp. 315–323. doi: 10.4161/cc.2.4.468.

Wu, H. *et al.* (1995) 'Generation of committed erythroid BFU-E and CFU-E progenitors does not require erythropoietin or the erythropoietin receptor.', *Cell*, 83(1), pp. 59–67.

Yamada, K. *et al.* (2005) 'Discrimination of Cell Nuclei in Early S-phase, Mid-to-late S-phase, and G 2 /M-phase by Sequential Administration of 5-Bromo-2 J -Deoxyuridine and 5-Chloro-2 J -Deoxyuridine', *The Journal of Histochemistry & Cytochemistry Journal of Histochemistry & Cytochemistry*, 53(11), pp. 1365–1370. doi: 10.1369/jhc.4A6601.2005.

Yano, M. *et al.* (1997) 'Expression and function of murine receptor tyrosine kinases, TIE and TEK, in hematopoietic stem cells.', *Blood*, 89(12), pp. 4317–26.

You, S. *et al.* (2011) 'Detection of BrdU-label retaining cells in the lacrimal gland: implications for tissue repair.', *Cell and tissue research*. NIH Public Access, 346(3), pp. 317–26. doi: 10.1007/s00441-011-1271-x.

Zetterberg, A. and Larsson, O. (1985) 'Kinetic analysis of regulatory events in G1 leading to proliferation or quiescence of Swiss 3T3 cells.', *Proceedings of the National Academy of Sciences of the United States of America*. National Academy of Sciences, 82(16), pp. 5365–9.

Zhang, L. *et al.* (2015) 'Long-term tracing of the BrdU label-retaining cells in adult rat brain', *Neuroscience Letters*, 591, pp. 30–34. doi: 10.1016/j.neulet.2015.02.023.

Zhang, P. *et al.* (2000) 'PU.1 inhibits GATA-1 function and erythroid differentiation by blocking GATA-1 DNA binding.', *Blood*, 96(8), pp. 2641–8.

Zhou, B. O. *et al.* (2014) 'Leptin-Receptor-Expressing Mesenchymal Stromal Cells Represent the Main Source of Bone Formed by Adult Bone Marrow', *Cell Stem Cell*, 15(2), pp. 154–168. doi: 10.1016/j.stem.2014.06.008.

Zhou, S. *et al.* (2001) 'The ABC transporter Bcrp1/ABCG2 is expressed in a wide variety of stem cells and is a molecular determinant of the side-population phenotype', *Nature Medicine*, 7(9), pp. 1028–1034. doi: 10.1038/nm0901-1028.

12 List of Publications

Publications with relation to the thesis

Páral P, Faltusová K, Molík M, Renešová N, Šefc L, Nečas E. Cell cycle and differentiation of Sca-1 + and Sca-1 − hematopoietic stem and progenitor cells. Cell Cycle. 2018;17(16):1979–91. doi: 10.1080/15384101.2018.1502573. **IF = 3.304**

Páral P, Báječný M, Savvulidi F, Nečas E. Cell Cycle Analysis Using In Vivo Staining of DNA-Synthesizing Cells. Methods Mol Biol. 2019. doi: 10.1007/7651_2019_228. **IF = 1.465**

Other publications

Hofer M, Pospíšil M, Hoferová Z, Komůrková D, Páral P, Savvulidi F, Sefc L. The pharmacological activation of adenosine A1 and A3 receptors does not modulate the long- or short-term repopulating ability of hematopoietic stem and multipotent progenitor cells in mice. Purinergic Signal. 2013;9(2):207–14. doi: 10.1007/s11302-012-9340-5. **IF = 3.19**

Loukotová L, Kučka J, Rabyk M, Höcherl A, Venclíková K, Janoušková O, Páral P, Kolářová V, Heizer T, Šefc L, Štěpánek P, Hrubý M. Thermoresponsive β-glucan-based polymers for bimodal immunoradiotherapy – Are they able to promote the immune system? J Control Release. 2017;268:78–91. doi: 10.1016/j.jconrel.2017.10.010. **IF = 7.877**

Faltusová K, Szikszai K, Molík M, Linhartová J, Páral P, Šefc L, Savvulidi F, Nečas E. Stem Cell Defect in Ubiquitin-Green Fluorescent Protein Mice Facilitates Engraftment of Lymphoid-Primed Hematopoietic Stem Cells. Stem Cells. 2018;36(8):1237–48. doi: 10.1002/stem.2828. **IF = 5.587**

13 Appendices

Appendix 1

Páral P, Faltusová K, Molík M, Renešová N, Šefc L, Nečas E. Cell cycle and differentiation of Sca-1 + and Sca-1 − hematopoietic stem and progenitor cells. Cell Cycle. 2018;17(16):1979–91. doi: 10.1080/15384101.2018.1502573.

Appendix 2

Páral P, Báječný M, Savvulidi F, Nečas E. Cell Cycle Analysis Using In Vivo Staining of DNA-Synthesizing Cells. Methods Mol Biol. 2019. doi: 10.1007/7651_2019_228.